Evidence for the Physical Interaction of Endosomes with Mitochondria in Erythroid Cells

Tanya Kahawita

Department of Physiology

McGill University, Montreal

June 2008

A thesis submitted to McGill University in partial fulfilment of the requirements of the degree of Master of Science

Your file Votre référence
ISBN: 978-0-494-67014-9
Our file Notre référence
ISBN: 978-0-494-67014-9

Abstract

Utilization of iron by hemoglobin-producing cells is highly efficient. The acquisition of iron from plasma requires the binding of diferric transferrin (Tf) to its cognate receptor (Tf-R) on the erythroid cell membrane, followed by internalization of the Tf - Tf-R complexes via receptor-mediated endocytosis. Through a poorly understood mechanism, iron is targeted to mitochondria, the site of heme biosynthesis. We believe that a direct interaction between iron-containing endosomes and mitochondria is essential for iron transfer to mitochondria and its efficient incorporation into heme.

In order to illustrate the interaction between endosomes and mitochondria, we have employed flow cytometry. Flow cytometry analysis of reticulocytes (erythrocyte precursors which still synthesize hemoglobin) stained with fluorescent dyes specific to mitochondria and endosomes revealed three distinct populations: mitochondria, endosomes and a population labeled with both dyes. This double-labeled population suggests a population composed of endosomes associated with mitochondria. Using non-fluorescent diferric-Tf, we were able to remove the double population, leaving only the endosomal and the mitochondrial population. This finding has confirmed that the double population is the result of the interaction between the two organelles.

Additionally, we established a cell-free assay consisting of fluorescent mitochondria and endosomes isolated from erythroid cells. Using confocal microscopy, we demonstrated a colocalization between the two organelles. We repeated the assay using fluorescent mitochondria and endosomes isolated from HeLa spinner cells. Using the mitochondrial uncoupler CCCP, we were able to significantly reduce the colocalization between the two organelles, indicating that the interaction between the organelles is specific and that the mitochondrial potential is a requirement for organellar interaction.

Based on our results from flow cytometry and confocal microscopy, we conclude that a specific and direct interaction exists between the two organelles.

Résumé

L'utilisation du fer (Fe) par les cellules productrices d'hémoglobine est très efficace. L'acquisition du fer à partir du plasma nécessite la liaison de la transferrine diferrique (Tf) à son récepteur apparenté (Tf-R) sur la membrane de cellules érythroïdes, suivi de l'internalisation du complexe Tf-Tf-R par endocytose. Par un mécanisme à ce jour inconnu, le fer est transporté vers les mitochondries, site de biosynthèse de hème. Nous croyons qu'une interaction directe entre les endosomes contenant le fer et les mitochondries est essentielle pour le transfert du fer aux mitochondries ainsi qu'à son incorporation efficace dans la hème.

Afin d'illustrer l'interaction entre les endosomes et les mitochondries, nous avons utilisé la cytométrie en flu. L'analyse par cytométrie en flu de reticulocytes (précurseurs d'érythrocyte qui synthétisent encore l'hémoglobine) marqués de colorants fluorescents spécifiques aux mitochondries et endosomes a dévoilé trois populations distinctes: mitochondries, endosomes et une population marquée avec les deux colorants. La population marquée des deux colorants suggère l'existence d'une population composée d'endosomes liés aux mitochondries. En utilisant le diferrique-Tf non fluorescent, nous avons réussi à supprimer la population marquée des deux colorants, laissant seulement la population endosomale et mitochondrique. Ces résultats confirment que la population marquée des deux colorants est le résultat de l'interaction entre les deux organelles.

De plus nous avons établi une analyse sans cellule composée de mitochondries et d'endosomes fluorescents isolés de cellules érythroïdes. En utilisant la microscopie confocale, nous avons réussi à démontrer une colocalization entre les deux organelles ce qui suggère une interaction spécifique. Nous avons également répété l'analyse en utilisant les mitochondries et les endosomes fluorescents isolés des cellules Hela Spinner. Utilisant le découpleur mitochondrique CCCP, nous avons réduit de manière significative la colocalization entre les deux organelles, ce qui indique que l'interaction entre les

organelles est spécifique et que le potentiel mitochondrique est nécessaire pour l'interaction entre organelles.

Basé sur nos résultats de cytométrie en flu et de microscopie confocale, nous concluons qu'une interaction spécifique et directe existe entre les deux organelles.

Acknowledgements

I would like to thank my supervisor Dr. Prem Ponka for his guidance and support throughout the length of this project and Dr. Matthias Schranzhofer, Dr. Alex Sheftel, Dr. Guanjun Nie and Dr. Tamara Bar-Magen for the many insightful discussions.

I am greatly indebted to Dr. Heidi McBride and the members of her laboratory who provided me with the knowledge and training to perform the cell-free assays. Additionally, Dr. McBride provided me with continual assistance and encouragement for which I am most grateful.

Sincere thanks to the members of my graduate committee, Dr. J. Presley, Dr. J. Orlowski, Dr. J.F. Prchal and Dr. J. Desbarats. A special thanks to Dr. Desbarats who introduced me to flow cytometry and who has provided with support both on a scientific and personal level.

A very special thanks to Dr. Judith Lacoste for her assistance with confocal microscopy and most importantly for taking the time to answer my many questions. Special thanks to Laurence Lejeune and Ken McDonald for their assistance with flow cytometry and to Dr. Vyoral for his technical assistance with regards to isolation of splenic erythroblasts.

I would like to sincerely thank Amanda Kasneci, Lila Kayembe, Dr. Matthias Schranzhofer, Dr. Tamara Bar-Magen, Shan Soe-Lin, Marc Mikhael and Daniel Santos Garcia for their unfailing support and encouragement throughout this rollercoaster that was my thesis.

Finally, a heartfelt thanks to my parents and brother whose love and relentless support has meant a great deal to me and has enabled me to complete yet another chapter in my life.

Table of Contents

List of Tables

List of Figures

Abbreviations

AGTF: Alexa Green Transferrin 488

ALA: 5-Aminolevulinic Acid

ALA-S: 5-Aminolevulinic Acid Synthase

APS: Ammonium Persulfate

Baf: Bafilomycin

CCCP: Carbonyl cyanide 3-chlorophenylhydrazone

DP : Dipyridyl

DMT1: Divalent Metal Transporter 1

EEA1: Early Endosomal Antigen 1

eIF4e: Eukaryotic Initiation Factor 4e

FB: Fusion Buffer

HES-DFO: Impermeant form of desferrioxamine

HT: Holo Transferrin

INH: Isonicotinic Acid Hydrazide

IRE: Iron Responsive Element

IRP: Iron Regulatory Protein

LIP: Labile Iron Pool

MB: Mitochondrial Isolation Buffer

MEL: Murine Erythroid Leukemia

MEM: Minimum Essential Media

MTDR: MitoTracker Deep Red 633

PBS: Phosphate Buffered Saline

PES: Post-Endosomal Supernatant

PMS: Post-Mitochondrial Supernatant

PNS: Post-Nuclear Supernatant

Rr(obs): Pearson Correlation Coefficient

Rr(rand): Pearson Correlation Coefficient following randomization

SA: Sideroblastic Anemia

SIH: Salicylaldehyde Isnoicotinoyl Hydrazone

SIM: Sucrose Imidazole Mannitol Buffer

Tf: Transferrin

Tf-R: Transferrin Receptor

TTBS: Tween Tris Buffer Saline

UTR: Untranslated Region

W-7: N-(6-Aminohexyl)-5-chloro-1- napthalenesulfonamide hydrochloride

YFP: Yellow Fluorescent Protein

Introduction

1.1. Systemic Iron Homeostasis

Iron is a precious metal involved in numerous biological functions such as DNA synthesis, oxygen transport and electron transfer, and is therefore indispensable for the growth and survival of an organism (Ponka, 2003). Iron exists in either the ferric (Fe^{3+}) or ferrous (Fe^{2+}) form; the ability of iron to exist in two oxidative states confers its versatility, while also resulting in its potential toxicity. Through Fenton chemistry, ferrous iron is readily oxidized to ferric iron by hydrogen peroxide and in the process generates highly reactive hydroxyl radicals (Fenton, 1876). The production of such radicals has deleterious consequences such as the peroxidative damage of lipid membranes, protein structures and nucleic acids (Ganz and Nemeth 2006). Furthermore, the ferric form is virtually insoluble at physiological pH as the concentration of aquated Fe^{3+} can not exceed 10^{-17} M (Halliwell and Gutteridge 1990). Therefore, the acquisition, absorption and storage of iron is carefully orchestrated in order to maintain body iron homeostasis and minimize iron toxicity. Fortunately, evolution has provided the organism with means to circumvent the element's potential toxicity and insolubility and ensure it's safe and efficient use. For instance, iron is always found complexed with a protein in order to minimize free iron, one such protein being Transferrin (Tf). Tf, a liver produced plasma glycoprotein binds tightly but reversibly to iron and transports the element from sites of absorption to sites of utilization and storage (Richardson and Ponka 1997). The total amount of iron contained within the body can be envisioned as several compartments designated

for storage, absorption and utilization. The small intestine is the site of iron absorption from the diet. Because humans posses a limited capacity to excrete iron, the small intestine represents a critical point of control. Therefore the homeostasis of body iron levels is dictated by iron absorption (Wintrobe, 1995). Approximately 1 mg /day is lost through non-specific mechanisms such as cell desquamation; therefore 1 mg is absorbed from the daily diet in order to maintain steady body iron levels. In healthy individuals, iron absorption can be modified in order to meet the demands of the organism dictated by both the amount of storage iron and the rate of erythropoiesis (Wintrobe, 1995).

Iron represents 55 and 45 mg per kilogram of body weight in adult men and women respectively (Ponka, 2003). At least two thirds of the body's iron content is contained within erythrocytes and their precursors (Andrews 2002) (Fig.1). Myoglobin, cytochromes and other iron-containing enzymes contain 10%, and the remaining 20-30% is stored in ferritin, a cytosolic iron storage protein (Ponka, 2002). Erythroid precursors are thus by far the most avid consumers of the metal. Erythropoiesis is a continual process which requires a relentless supply of iron for the production of hemoglobin. The iron demands of erythropoiesis can not be met by the miniscule amount of iron absorbed daily through the intestine. Consequently, iron present in hemoglobin of senescent erythrocytes must be recycled and reincorporated into new erythrocytes. The recycling of iron is executed exclusively by specialized macrophages found primarily in the liver, spleen and bone marrow and are collectively referred to as the reticuloendothelial system (Knutson and Wessling-Resnick 2003), where senescent erythrocytes are

identified, engulfed and degraded. Iron is returned to the plasma complexed to Tf in its ferric form and then shuttled to the bone marrow, the site of erythropoiesis. Interestingly, iron bound to Tf is less than 0.1% of total body iron (3mg), however it is the most dynamic iron pool, possessing the highest rate of turnover (Ponka, 2002). In 24 hours, Tf delivers 30 mg of iron to various sites in the body, 80% of which is delivered to the bone marrow for erythropoiesis (Sheftel, 2006).

1.2. Cellular Iron Acquisition

In normal circumstances, nearly all plasma iron is bound to Tf, the iron binding protein which circulates the element to its various sites within the body. Cellular iron acquisition is mediated by the transferrin receptor (Tf-R); Tf binds to its cognate receptor on the cell membrane and is subsequently internalized via receptor mediated endocytosis (Fig. 2). With the exception of enterocytes, macrophages and mature erythrocytes, all cells acquire iron via Tf. Diferric Tf binds to the Tf-R on the cell membrane by a physicochemical interaction that does not require temperature and energy. In contrast, endocytosis is temperature and energy dependant process. Once diferric Tf and its cognate receptor are internalized, the pH of the endosomal compartment is considerably reduced by an uncharacterized adenosine triphosphate-dependant proton pump. The decrease in pH is sufficient to strip the element from the receptor-ligand complex and the metal is then released into the endosome. The export of iron from the endosomal compartment is facilitated by the divalent metal transporter 1 (DMT1); however, the iron must be in the ferrous form in order to be exported (Gunshin, Mackenzie et al. 1997). Therefore, iron is reduced prior to its egress from the endosomes by a

ferricreductase. Recently, a putative ferricreductase, Steap-3, was identified (Ohgami, Campagna et al. 2005). The enzyme is reported to be expressed in the endosomes of erythroid precursors and co-localizes with Tf and its receptor in endosomes. Following its exit from the endosome, iron can enter into functional compartments within the cell or can be stored in ferritin, a large multimeric cytoplasmic iron storage protein (Harrison and Arosio 1996). The storage of iron in ferritin protects the cell from the damaging effects of free iron and sequesters the iron in a bioavailable form (Napier, Ponka et al. 2005). The now iron-free Tf, apo-Tf, still bound to the Tf-R, is returned to the cell membrane where it is released from the cell and returned to the plasma.

1.3. Iron Metabolism in Erythroid Cells

Iron is an invaluable constituent of hemoglobin; the oxygen transport properties of the protein are conferred by the element. Hemoglobin is comprised of four globin polypeptide chains each covalently linked to an iron-containing heme prosthetic group. Iron metabolism in erythroid cells is an intricate process which requires the proper coordination and communication between several processes. Briefly, iron is acquired via Tf and Tf-R, and once internalized, iron is targeted to the mitochondria which is the site of heme biosynthesis. Globin mRNA is translated on polysomes in the cytoplasm. Once heme is synthesized, it is exported from the mitochondria into the cytoplasm where it is combined with globin to form hemoglobin. The acquisition of iron and its incorporation into heme by hemoglobinizing cells are unique and refined processes due in part to the distinct regulation of the specific proteins involved.

1.3.1. Iron acquisition via Transferrin

The iron Tf delivery system operates with remarkable efficiency. Erythrocytes contain approximately 45,000-fold more heme iron (20 mmol/L) than non-heme iron (440 nmol/L) (Richardson and Ponka 1997). Therefore, virtually all Tf-iron accepted by erythroid cells is incorporated into heme; negligible amounts of non-heme iron are left within mature erythrocytes (Ponka, 2002). Thus, iron-Tf delivery is highly efficient and suggests an intimate link between iron acquisition and heme biosynthesis.

Erythroid cells are stringently dependant on iron derived from Tf. The latter has been confirmed by both in vitro and in vivo studies. Hereditary atransferrinemia, also known as congenital hypotransferrinemia, is a rare disorder characterized by microcytic anemia and iron overload. Since its identification in 1961, a total of 10 patients have been reported (Aslan, Crain et al. 2007). Anemia in such patients can be alleviated via infusion with human plasma or purified Tf. Similarly, mice that are homozygous for atransferrinemia suffer from severe anemia and die shortly after birth unless treated with exogenous Tf or transfused with red blood cells (Trenor, Campagna et al. 2000). Therefore both human and murine examples of the disorder emphasize the absolute requirement of Tf-derived iron by erythroid cells.

1.3.2. Transferrin Receptor

The Tf-R, like Tf is a significant element of iron acquisition by the erythroid cell and its importance is exemplified in Tf-R knockout mice. Homozygous mice completely devoid of the Tf-R die *in utero* whereas heterozygotes develop

hypochromic, microcytic anemia. The expression of Tf-R on erythroblasts of heterozygotes is reduced in comparison with the wild type. Therefore, transcription of both copies of the gene is absolutely required for normal hemoglobinization (Levy, Jin et al. 1999).

Regulation of the Tf-R differs between erythroid and non-erythroid cells. In erythroid cells, regulation occurs post-transcriptionally by an elegant system comprised of cytosolic iron regulatory proteins (IRP1 and IRP2), and key nucleotide sequences known as iron-responsive elements (IRE) (Kuhn 1994). The IREs are stem loop structures located in the untranslated regions (UTR) of various mRNAs encoding proteins involved in iron metabolism. IRPs will bind to these stem loop structures under certain conditions and depending on the location of the UTR will either inhibit or promote tranlation. Tf-R and erythroid 5-aminolevulinic acid synthase (ALA-S) posses IREs located in the 3'-UTR and 5'-UTR respectively (Theil, McKenzie et al. 1994). Cellular iron levels are closely monitored by the IRP-IRE system. Tf-R mRNAs in non-erythroid cells are sensitive to cellular iron levels which alter the affinity between the IREs and IRPs. In iron replete conditions, IRP1 possesses aconitase activity conferred by an iron-sulfur cluster which inhibits IRE binding. Consequently, the Tf-R mRNA is unstable and along with IRP-2 is degraded. When intracellular iron levels are low, the iron-sulfur cluster of IRP-1 dissociates, resulting in a conformation change and thus permitting IRE binding (Schalinske, Anderson et al. 1997). The binding of IRP-1 to the IRE stabilizes the Tf-R mRNA, and thus facilitates an increased expression of Tf-R.

In contrast, erythroid cells appear refractory to fluctuating intracellular iron levels. Using murine erythroid leukemia (MEL) cells, investigators examined the sensitivity of Tf-R expression to iron. Induced differentiation of MEL cells resulted in an increase in transcription of the Tf-R gene. The investigators did not note an increase in the activity of IRP in induced MEL cells; rather, they observed that the stability of the Tf-R mRNA was only slightly affected by excess iron concentrations (Chan, Seiser et al. 1994). Therefore, Tf-R expression appears to be indifferent to fluctuating levels of cellular iron perhaps as a result of the greatly increased rates of transcription of the Tf-R gene (Ponka 1999).

1.3.3. 5-Aminolevulinic Acid Synthase (ALA-S)

Heme production in immature erythroid cells occurs at an astonishing rate; on a per-cell basis, the rate of heme synthesis is at least an order of magnitude greater than the liver, the second highest heme producer in the organism (Ponka, Sheftel et al. 2002). The difference in rate of production of heme between erythroid and non-erythroid cells is attributed to the acquisition of iron and to ALA-S, an enzyme of the heme biosynthesis pathway.

Heme is assembled by a complex series of enzymes in the mitochondrion and cytosol (Fig. 3). The first step involves the condensation of succinyl CoA and glycine by 5-aminolevulinic acid (ALA) synthase to produce ALA. ALA is transferred to the cytosol where a sequence of reactions yields a ring structure known as coproporphyrinogen III. This molecule then returns to the mitochondria where it undergoes several additional reactions to eventually produce protoporphyrin IX. Lastly, the insertion of iron into the ring structure of the

protoporphyrin IX is catalyzed by ferrochelatase. ALA synthase (ALA-S) is of particular importance in both erythroid and non-erythroid cells because it serves as critical point of regulation.

Two different genes encode for the ALA-S enzyme: one of these genes is expressed ubiquitously (ALA-S1) while the other is specific to erythroid cells (ALA-S2). The synthesis of the ALA-S1 gene is feedback inhibited by heme in non-erythroid cells and is thus the rate-limiting step of heme biosynthesis. On the contrary, ALA-S2 is not regulated by heme; at the level of translation, the ALA-S2 gene contains an IRE, a conserved sequence of 28 nucleotides located at the 5' untranslated region of the mRNA. The binding of the IRP to the IRE gives rise to the IRE/IRP complex located at the 5' UTR of the erythroid ALA-S2 mRNA. Formation of the complex inhibits the binding of ribosomes and prevents translation. With increasing levels of intracellular iron, the affinity between the IRE and its respective binding protein is altered, thus permitting ribosomes and initiation factors to bind. Hence, the translation of the ALA-S2 mRNA is regulated by the availability of iron which, by definition, means that iron supply to erythroid cells is limiting and controlling factor in heme synthesis in these cells.

In fact, the above conclusion was made earlier, exploiting a membrane permeable iron chelate, iron salicylaldehyde isonicotinoyl hydrazone (Fe-SIH), which can deliver iron to the cell independently of the Tf and Tf-R pathway (Ponka and Schulman, 1985). Heme synthesis was compared in erythroid cells treated with saturating concentrations of iron-bound Tf (20 μM) or treated with

Fe-SIH at 100 μM. The investigators reported a significant increase in the heme synthesis of erythroid cells treated with the iron chelators in comparison with those cells treated with iron-bound Tf (Ponka and Schulman, 1985; Laskey, Ponka et al. 1986) Therefore, the rate of iron acquisition from Tf dictates the rate of heme synthesis in erythroid cells. Although heme biosynthesis is regulated by iron acquisition, non-committed heme inhibits the acquisition of iron from Tf and thus regulates the rate of heme synthesis. Therefore, the latter is a feedback mechanism which ensures that the rate of iron uptake does not exceed its rate of incorporation into heme (Ponka 1999). Overall, because erythroid cells produce vast amounts of hemoglobin, iron acquisition and heme production are tightly coupled in order to avoid accumulation of toxic intermediates such as protoporphyrin IX.

1.3.4. Mitoferrin

Insertion of iron into protoporphyrin IX by ferrochelatase requires the entry of iron into the mitchondria. Import of the element is facilitated by the recently identified protein mitoferrin, a mammalian homolog of the mitochondrial solute carrier proteins 3 (MRS3) and MRS4 which are partly responsible for iron acquisition in yeast (Shaw, Cope et al. 2006). A mutation in the *mitoferrin* gene was responsible for the zebrafish mutant, *frascati*, which exhibited hypochromic anemia and impaired mitochondrial iron uptake. It was demonstrated that the *frascati* mutant could be rescued by introduction of the gene encoding murine mitoferrin (Shaw, Cope et al. 2006). Erythroblasts generated from murine embryonic stem cells null for *mitoferrin* displayed maturation arrest and reduced

incorporation of ^{55}Fe into heme. Together, these findings identify mitoferrin as a mitochondrial iron importer essential for proper heme biosynthesis.

1.3.5. The Labile Iron Pool

The fate of iron following its exit from endosomes in erythroid cells is subject to great debate. Ultimately, iron must traverse both mitochondrial membranes in order to be inserted by ferrochelatase into protoporphyrin IX. The intermediate steps of this journey have been discussed in excess over forty years. Currently, it is generally believed that following iron's release from endosomes, iron enters the cytosol where it equilibrates with a low molecular weight labile iron pool (LIP) (Fig.2). The iron in the intermediate pool can then supply iron to sites of utilization (Jacobs 1977). It has been suggested that iron will bind to peptides, proteins and nucleotides; however, this has not been shown unequivocally (Jacobs 1977). Several publications printed in the 1960's suggested the existence of a protein intermediate bound to iron that was a non-heme form and distinct from ferritin (Greenough, Peters et al. 1962; Zail, Charlton et al. 1964; Primosigh and Thomas 1968). The iron-bound intermediate however was neither characterized nor identified. In contrast, in erythroid cells incubated with ^{59}Fe, virtually no ^{59}Fe was present in a non-Tf or non-heme form (Martinez-Medellin and Schulman 1972; Zhang, Sheftel et al. 2005) suggesting that such an iron-carrier intermediate probably does not exist. More recent studies with erythroid cells have provided further evidence contrary to the idea of the LIP and the belief that iron, by an unknown mechanism, freely diffuses to the mitochondria.

1.3.6. Evidence for Targeting of Endosomal Iron to the Mitochondria

In erythroid cells, evidence exists that iron is specifically targeted to the mitochondria. Iron acquisition by erythroid cells occurs with a high efficiency; following a three minute incubation of reticulocytes with ^{59}Fe-Tf, about 80 % cell-associated iron can be found in heme (Richardson, Ponka et al. 1996). The rapidity of iron's incorporation into heme could be attributed to the specific targeting of iron towards the mitochondria in erythroid cells. In hemoglobinizing cells, the vast majority of iron taken in is directed to the mitochondria for the purpose of heme biosynthesis. Studies in erythroid cells have demonstrated that when heme synthesis is suppressed using isonicotinic acid hydrazide (INH) or succinylacetone, iron derived from Tf continues to flow into the mitochondria (Borova, Ponka et al. 1973; Ponka, Wilczynska et al. 1982; Richardson, Ponka et al. 1996). In contrast, in non-erythroid cells, iron exceeding the metabolic needs of the cell is stored in ferritin. These findings further emphasize the unique mechanisms in place by erythroid cells. The results provided by in vitro studies are confirmed by individuals diagnosed with X-linked sideroblastic anemia (SA). The disorder is characterized by the accumulation of iron within the mitochondria of erythroblasts. The iron-loaded mitochondria of SA patients contain dense, ring-shaped structures and are thus called "ringed sideroblasts". X-linked SA is the most common inherited SA and is the result of mutations in the ALA-S2 gene which have been known to reduce the activity of the ALA-S2 enzyme (McLintock and Fitzsimons 2002). Therefore, both *in vitro* and *in vivo* examples provide evidence that endosomal iron is targeted to the mitochondria.

1.3.7. A New Model of Intracellular Iron Transport in the Erythroid Cell

A new model of intracellular iron transport within erythroid cells has been proposed to account for the fact that: incorporation of iron into heme occurs with extreme efficiency; no cytoplasmic iron transport intermediate has been identified, and lastly evidence exists that endosomal iron is targeted to the mitochondria. The model suggests that following iron's release from Tf within endosomes, it is handed directly from endosomal protein to mitochondrial protein and remains protein-bound until it reaches ferrochelatase in the mitochondria, its final point of destination (Ponka 1997). The transfer of iron from the endosome to the mitochondria may require direct interaction between the organelles (Fig. 4). Recent publications produced by our laboratory have provided evidence supporting this hypothesis (Zhang, Sheftel et al. 2005). The study sought to investigate the involvement of endosomes in the targeting of iron to mitochondria. In order to eliminate the possible effects of various agents on endocytosis, the investigators designed a protocol which permitted the creation of a cohort of ^{59}Fe-Tf labeled endosomes within reticulocytes. The incorporation of ^{59}Fe into heme was closely followed under specific conditions in order to determine the requirements necessary for incorporation of iron into heme. Using membrane-permeable ferrous (dipyridyl, DP) and ferric (salicylaldehyde isnoicotinoyl hydrazone, SIH) iron chelators, the investigators demonstrated that both chelators could intercept the transfer of endosomal ^{59}Fe to protoporphyrin IX when reticulocytes were incubated at 37°C. However when the chelators were added during the lysis of ^{59}Fe reticulocytes at 4°C, virtually no ^{59}Fe chelates were

formed. Therefore inhibition of incorporation of ^{59}Fe into heme and formation of ^{59}Fe chelates could only occur when the cells were actively metabolizing the element. Furthemore, addition of the myosin light-chain kinase inhibitor, wortmannin, as well as the calmodulin antagonist, W-7, caused significant inhibition of ^{59}Fe incorporation from ^{59}Fe-Tf labeled endosomes into heme. Both reagents are known to inhibit the microfilament motor, myosin, which is involved in the intracellular movement of endosomes. The decreased ^{59}Fe incorporation into heme caused by inhibitors of intracellular endosomal trafficking provide evidence against the current belief that iron enters a "freely diffusible" pool in the cytosol. These results suggest that the translocation of iron from the endosome to the mitochondria requires an association between the two organelles.

In a separate study conducted by the same investigators, it was determined that iron from Tf-containing endosomes bypass the cytosol (Sheftel, Zhang et al. 2007). Reticulocytes were loaded with a membrane impermeant form of the iron chelator desferrioxamine (HES-DFO) and then incubated with $^{59}Fe_2$-Tf. In comparison with control reticulocytes devoid of the cytoplasmic chelator, HES-DFO loaded reticulocytes incorporated an equivalent amount of $^{59}Fe_2$-Tf into heme. Therefore, the chelator was unable to intercept the Tf-borne ^{59}Fe. This finding confirmed that iron derived from Tf-containing endosomes can bypass the cytosol and can reach the mitochondria without entering a chelatable cytoplasmic pool. In addition, live confocal microscopy studies of fluorescently labeled endosomes and mitochondria of reticulocytes revealed transient interactions

between endosomes and mitochondria of erythroid cells (Sheftel, Zhang et al. 2007).

1.4. Rationale of Studies

Iron assimilation in erythroid cells is a unique and refined process. Erythroid cells utilize and incorporate iron with remarkable efficiency, in part due to the targeting of endosomal iron to the mitochondria. Recent evidence revealing that iron-laden endosomes completely bypass the oxygen rich cytosol and deliver iron to the mitochondria weakens the widely accepted theory of the existence of a LIP (Sheftel, Zhang et al. 2007). Given the oxygen rich cytosol of erythroid cells and the potential toxicity of the element, the unleashing of the element into such a milieu would be catastrophic. Trace amounts of free iron in combination with cellular reducing equivalents have been demonstrated to oxidize hemoglobin (Scott and Eaton 1995). The findings suggest that a pool of free iron is capable of establishing a self-amplifying and self-propagating redox reaction with hemoglobin that can eventually result in red cell destruction. Additionally, transient interactions between endosomes and mitochondria, as seen by confocal microscopy, suggest that endosomes are employed in the shuttling of iron to the mitochondria. My work examines the possibility that direct interaction between iron containing endosomes and mitochondria is essential for iron transfer to mitochondria and its efficient incorporation into heme.

2. Materials and Methods

2.1. Materials

2.1.1. Chemicals and Reagents

Nitrocellulose membranes were purchased from Pall Life Science (East hills, NY). Acrylamide/bis (37.5:1) 40%, TEMED and ammonium persulfate (APS) were purchased from BioShop (Burlington, Ontario). ECL western blotting detection reagent was purchased from GE Healthcare (Piscataway, NJ). Porin antibody was purchased from Calbiochem (EMD, Madison WI). Early endosomal antigen 1 (EEA1) antibody was purchased from Upstate (Millipore, Billerica MA). Eukaryotic initiation factor 4e (eIF4e) antibody was purchased from Cell Signaling (Danvers, MA). Secondary antibodies were purchased from Zymed (Invitrogen, Carlsbad, CA). MitoTracker Deep Red 633 (MTDR) and Alexa Green Transferrin 488 (AGFT) were purchased from Molecular Probes (Invitrogen, Carlsbad, CA). Protease inhibitor was purchased from Roche (Penzberg, Germany). Pronase was purchased from Boehringer Mannheim (Mannheim, Germany). Holo-transferrin (referred to as non-fluorescent diferric-transferrin), deoxyribonuclease I, (DNase I) and N-(6-Aminohexyl)-5-chloro-1-napthalenesulfonamide hydrochloride (W-7), carbonyl cyanide 3-chlorophenylhydrazone (CCCP), Guanosine 5'-triphosphate lithium salt (GTP), and adenosine 5'-triphosphate disodium salt (ATP) and New Methylene Blue were purchased from Sigma-Aldrich (St.Louis, MO). Bafilomycin was purchased from Bioshop (Burlington, Ontario). Fluorescent mounting media was purchased from Dako (Glostrup, Denmark). Microslides and micro coverslips were

purchased from VWR (West Chester, PA). A Wheaton dounce homogenizer was purchased from Fisher Scientific (Waltham, MA).

2.1.2. Required Materials for Studies with Erythroid Cells

All reticuloctye incubations were performed in Minimum Essential Media (MEM, Invitrogen, Carlsbad, CA) supplemented with 1% bovine serum albumin (BSA), 25 mM HEPES, and 10 mM Sodium Bicarbonate, pH 7.4. Mitochondrial isolation buffer (MB) was used to isolate splenic erythroblasts. The MB consisted of 220 mM mannitol, 68 mM sucrose, 20 mM HEPES pH 7.4, 80 mM KCl, 0.5 mM EGTA, 2 mM magnesium acetate, and protease inhibitors. The endosomal isolation buffer (SIM) consisted of 250 mM sucrose, 3 mM imidazole, 1 mM magnesium chloride and protease inhibitors. The 40x fusion buffer (FB), consisted of 700 mM sucrose, 1.5 mM KCl, 10 mM EGTA, 40 mM magnesium acetate, and 200 mM HEPES at pH 7.4.

2.1.3. Instruments

Flow Cytometry was performed using the Becton Dickinson FACSAria sorter and microscopy was performed with a Zeiss LSM 5 Pascal confocal inverted microscope.

2.2. Animals

Female CD-1 retired breeders were purchased from Charles River Laboratories (Wilmington, MA) and housed in microisolator cages.

2.3. Methods

2.3.1. Isolation of Reticulocytes

Blood was extracted from CD-1, female mice that had been treated for three consecutive days with 50mg/kg of phenylhydrazine administered intraperitoneally. Mice were permitted to recover for 2-3 days and were bled on day 6 or day 7 following the first injection. Blood was obtained via cardiac puncture using a heparinized syringe. The use of Phenylhydrazine and this specific time course allowed us to collect blood that contained 30 % reticulocytes as verified by new methylene blue staining. These samples will now be referred to as "reticulocytes".

2.3.2. Flow Cytometry

Reticulocytes were washed 3 times with ice cold PBS and the buffy coat removed. All wash steps used ice cold PBS and samples were centrifuged at 750g for 5 minutes at 4°C. The cell pellet was resuspended in 4 mL of MEM and divided into four samples, with each sample labeled with Alexa Green Transferrin 488 or MitoTracker Deep Red 633, both or neither. Therefore, the sample labeled with Alexa Green Transferrin 488 was used for the Alexa Green Transferrin time course and served as a positive control for the fluorophore and will be referred to as the AGTF sample. The sample labeled solely with MitoTracker Deep Red 633 served as a positive control for the dye and will be referred to as the MTDR sample. The sample serving as a negative control without any fluorophores will be referred to as the Control sample. The sample labeled with both MitoTracker

Deep Red 633 and Alexa Green Transferrin will be referred to as the Double sample.

2.3.2.1. MitoTracker Deep Red Positive Control

The MTDR sample was resuspended to a final volume of 15 mL with MEM and incubated with MitoTracker Deep Red 633 at 500 nM for 30 minutes at 37°C in a shaking waterbath. Cells were then washed with PBS and centrifuged at 750g for 5 minutes at 4°C three times.

2.3.2.2. Alexa Green Transferrin Positive Control and Time Course

Prior to the addition of the flurophore, the sample was resuspended to a final volume of 5 mL with MEM and incubated at 37°C for 45 minutes in a shaking waterbath in order to free transferrin receptors of unlabeled transferrin. The sample was then washed 3 times with PBS. The pellet was resuspended in 10 mL of MEM and incubated for one hour on ice with Alexa Green Transferrin 488 at 500 nM. The AGTF sample was then divided into eight time points (0', 1', 5', 15', 30', 60') (Fig. 5). For each time point, 500 µl of the AGTF cell suspension was added to 500 µl of pre-warmed MEM containing 5 µM of Alexa Green Transferrin 488. Samples were incubated at 37°C in a shaking water bath for the allotted time. Following incubation, each time point was promptly removed from the water bath, placed on ice and diluted with ice cold PBS. Each time point was washed two times with PBS. All samples were resuspended in 1 mL of MEM and treated for 30 minutes on ice with Pronase (1mg/mL) in order to remove any

fluorescent probe bound to transferrin receptor present on the cell surface. Following Pronase treatment, cells were washed three times with PBS.

2.3.2.3. Time Course of Double-Labeled Reticulocytes

The sample was incubated first with MitoTracker Deep Red 633 in the same manner as the MTDR positive control and following the final wash with PBS, was resuspended in 10 mL of MEM and incubated with Alexa Green Transferrin 488 (500 nM) for one hour on ice (Fig.6). The sample was then divided into eight aliquots in preparation for the time course (0', 1', 5', 15', 30', 60', 90'). For each time point, 500 µl of the AGTF cell suspension was added to 500 µl of pre-warmed MEM containing 5 µM of Alexa Green Transferrin 488. Samples were incubated at 37°C in a shaking water bath for the allotted time. Following its incubation, each time point was promptly removed from the water bath, placed on ice and diluted with ice cold PBS. Each time point was washed two times with PBS. All time points were resuspended in 1 mL of MEM and treated for 30 minutes on ice with Pronase (1mg/mL) in order to remove any fluorescent probe bound to the transferrin receptor on the cell surface. Samples were then washed three times with PBS.

2.3.2.4. Treatment of Double-labeled Reticulocytes with Non-Fluorescent Diferric Transferrin

Following the double-labeled time course, time point 30 was washed twice with PBS and the cell pellet resuspended in 10 mL of MEM. The cell suspension was

then divided into five time points, 1 mL was used for each time point i.e.0', 5', 30' 60', 120' (Fig. 7A & 7B). Each time point was added, excluding time point 0, to 4mL of pre-warmed MEM, which contained 10 uM of non-fluorescent diferric transferrin and was placed in a 37°C shaking waterbath for the prescribed amount of time. Following its incubation, each time point was immediately removed, placed on ice and followed by the addition of ice cold PBS. Each time point was washed 3 times with PBS and then resuspended in 1 mL of MEM to which was added 1mg/mL of Pronase. The samples were kept on ice for 30 minutes and were then washed 3 times with PBS.

2.3.2.5. Treatment of Double-Labeled Reticulocytes with Inhibitors

Bafilomycin, an inhibitor of v-ATPase responsible for endosomal acidification (Zhang, Sheftel et al. 2005; Finbow and Harrison 1997), was added to reticulocytes labeled already with MitoTracker Deep Red 633 (Fig.8). More specifically, the inhibitor was added midway through the 1 hour incubation of the reticulocytes with Alexa Green Transferrin 488. Following the 1 hour incubation, reticulocytes were incubated at 37°C in a shaking water bath for 30 minutes in pre-warmed MEM media containing 5 μM of Alexa Green Transferrin 488. Following the incubation at 37°C, samples were removed, immediately placed on ice and diluted with cold PBS. Cells were then washed twice with PBS, treated with Pronase (1mg/mL) for 30 minutes at 4°C and washed three times with PBS. The above method was repeated using W-7, a calmodulin antagonist

(Bourguignon, Gunja-Smith et al. 1998; Ito, Tanabe et al. 1989). All experiments with inhibitors were repeated three times.

2.3.2.6. Flow Cytometry Analysis

All samples, positive and negative controls and all single and double label time points including time points treated with non-fluorescent diferric transferrin and samples treated with inhibitors, were resuspended in 1 mL MB buffer and were subjected to rapid freeze and thaw lysis. Samples were spun at 800g for 10 minutes at 4°C; the supernatant of each sample was removed and kept on ice for analysis via flow cytometry. Fluorescence signals were determined immediately using a FACSAria sorter from Becton Dickinson equipped with an argon and red laser emission of 488 and 633 nm respectively. Alexa Green Transferrin 488 and MitoTracker Deep Red 633 were identified by using a 530/30 and a 660/20 band pass filter respectively. Logarithmic fluorescence as well as forward and side scattered light were collected. The analysis was performed using FCS Express V3 software.

2.3.3. Erythroid Cell-Free Assay

2.3.3.1. Isolation of Fluorescent Early Endosomes from Reticulocytes

Reticulocytes were isolated from a CD-1 phenylhydrazine-treated mouse as previously described. The cells were washed three times with phosphate buffered saline (PBS) at 750g for 5 minutes at 4°C followed by removal of the buffy coat. The pellet was resuspended in MEM and the suspension was incubated at 37°C

for 45 minutes in a shaking water bath. The reticulocytes were then washed three times with ice-cold PBS. The cell pellet was resuspended in 30 mL of MEM (approximately 10 billion cells/mL), and incubated with AGTF at 500nM for one hour on ice. Following the incubation, the cell suspension was added to pre-warmed (37°C) MEM and incubated for 5 minutes in a 37°C shaking water bath in order to create a cohort of AGTF labeled early endosomes. Following the five minute incubation, endocytosis was immediately halted by the addition of ice cold PBS and the cells were placed on ice. Excess fluorescent probe was removed by washing the cells 3 times with ice cold PBS. The cell pellet was resuspended in 5 mL of MEM and treated with Pronase (1mg/mL) for 30 minutes at 4°C. The suspension was then washed 3 times with ice cold PBS.

The cell pellet was resuspended in 2 cell pellet volumes of SIM and following the addition of 1x protease inhibitor, cells were lysed via rapid freezing in liquid nitrogen and thawing at 4°C. Unbroken and lysed cells were pelleted at 800g for 10 minutes at 4°C. The supernatant was removed and set aside on ice. The pellet was resuspended in SIM buffer to which protease inhibitor was added and lysed once again via rapid freezing and thawing (F/T). Supernatants were pooled from both F/T cycles and were centrifuged at 20,000g for 20 minutes in a SW55Ti Beckman rotor at 4°C. The post-nuclear supernatant (PNS) was separated from the pellet and re-centrifuged at 60,000g for 1 hour at 4°C in the same rotor. The endosomal pellet was then resuspended in SIM buffer and frozen at -135°C for later use. 100 µl of the post-endosomal supernatant (PES) was set aside for western blot analysis.

2.3.3.2. Isolation of Mitochondria from Splenic Erythroblasts

Mitochondria were isolated from the splenic erythroblasts of female CD-1 mice treated with phenylhydrazine and sacrificed as described above. The spleen was removed and placed in 4 mL of ice cold PBS and 1 mL of DNase I (1mg/mL). The spleen was disrupted with scissors into 2 x 2 mm pieces over ice and passed 6 times through a 10 mL plastic syringe. The suspension was filtered through a fine metal mesh into a 50 mL Falcon tube and centrifuged at 4°C for 5 minutes at 1000g. 4 mL of PBS and 1mL of DNase I (1mg/mL) were added to the cell pellet; the tube was kept on ice for 20 minutes and vortexed every 5 minutes to release DNA from clumped cells. The suspension was adjusted to a final volume of 50 mL with ice cold PBS and filtered once more through the fine metal mesh and centrifuged at 1000g for 5 minutes at 4°C.

The cell pellet containing erythroblasts was resuspended in 800 µL of ice cold MB with the addition of 200 µL of DNase I (1mg/mL) and protease inhibitor. The cells were disrupted on ice using a teflon tight fitting pestle and a Wheaton 1mL mortar. Cell lysis was verified under a microscope by mounting 5 ul of the suspension; approximately 250 passes were necessary in order to obtain 70% lysis. The suspension was spun at 800g for 20 minutes at 4°C using a tabletop centrifuge. The nuclear pellet and post-nuclear supernatant (PNS) were separated. The PNS was spun at 800g for 10 minutes at 4°C in order to remove any residual contaminating nuclear fraction. The nuclear pellet was resuspended in 5 mL of MB in a 15 mL falcon tube and centrifuged at 800g for 10 minutes at 4°C. The supernatant was removed and pooled with the above mentioned PNS

fraction. The pooled PNS fraction was then spun at 9000g for 20 minutes at 4°C. The mitochondrial pellet was resuspended in 50 µl of MB; 100 µl of the post-mitochondrial supernatant (PMS) was reserved for western blot analysis.

2.3.3.3. Isolation of Cytosol from Reticulocytes

Reticulocytes were obtained from CD-1 female mice in the same manner as mentioned above. The cells were washed 3 times in ice cold PBS and the buffy coat removed. The cell pellet was resuspended in 2 cell volumes of SIM and prior to lysis via F/T, protease inhibitor was added to the suspension. Following the thawing of the cell suspension, cells were spun at 267,000g for 30 minutes at 4°C using a SW55 Ti Beckman rotor.

2.3.3.4. Preparation of Erythroid Cell-Free Assay

The cell-free assay consisted of 37 µg of mitochondrial protein obtained from erythroblasts, 74 µg of endosomal protein, cytosol 1 mg/mL, 1 mM of GTP, 1 mM of Sodium Succinate/ATP mix, 0.5 µl of 0.1 mM MTDR dye. Lastly, 1X FB was added in order to obtain a final reaction volume of 50 µl. The 10x sodium succinate/ATP mix consisted of 10 mM ATP, 50 mM sodium succinate, 0.8 mM ADP, 20 mM potassium phosphate dibasic; the pH was adjusted to 7.4 with potassium hydroxide. The components of the assay were added in no particular order with the exception of the mitochondria which was added last. Following the addition of all components, the sample was incubated for 15 minutes at 37°C on a

heating block. The reaction was immediately halted by placing the sample on ice and adding 200 µl of ice cold 1X FB.

2.3.4. HeLa Cell-Free Assay

Fluorescent endosomes and mitochondria isolated from HeLa cells were generously provided by Dr. Heidi McBride. Endosomes were labeled with Cy-5 transferrin, a fluorescently labeled form of transferrin. Mitochondria were isolated from HeLa cells transfected with yellow fluorescent protein (YFP) which was expressed specifically in the mitochondria.

2.3.4.1 Preparation of HeLa Cell-Free Assay

The cell-free assay was performed as previously described however using organelles and cytosol isolated from HeLa cells. Additionally, the assay was repeated with the addition of the mitochondrial uncoupler, CCCP at a concentration of 4 µM. In order to evaluate the assay, 200 mitochondria were counted in total per assay. The number of total mitochondria in contact with endosomes was counted as well. These values were used to determine the percentage of total mitochondria in contact with endosomes

2.3.5. Confocal Microscopy

50 µl of cell-free assay sample was mixed with 50 µl of Dako mounting medium and 40 µl of the mixture was mounted on microscope slides. Slides were kept at 37°C for 15 minutes and then at 4°C for 30 minutes. Slides were placed on the

stage of a Zeiss LSM 5 Pascal confocal inverted microscope that had been outfitted with a 63x/1.4 NA objective. Using the Zeiss LSM 510 software, a multi-channel protocol was used to scan the sample for each fluorochrome as described below.

Mitochondria, labeled with MTDR, were detected in the first track using a 5mW HeNe 633nm line (10-14%), HFT 448/543/633 and a long-pass filter (LP650). Endosomes, labeled with AGTF, were detected in the second track using a 30mW argon 488nm line (1-25%), HFT 488 and band-pass filter of 505-560. The pinhole diameter was set to 1 Airy unit for the green emission. Both channels were sampled at an optical thickness of 0.9 um. YFP-labeled mitochondria and Cy-Transferrin labeled endosomes derived from HeLa cells were detected using the above-mentioned lasers, filters and settings.

2.3.5.1. Data Analysis of Erythroid Cell-Free Assay

Preliminary colocalization analyses were performed using the open source image processing software ImageJ (Rasband, 2004). Background was first removed using the plugin ROI/BB subtraction from region of interest (ROI). An intensity correlation coefficient-based analysis was next performed by calculating the Pearson's correlation coefficient (R_r) (Manders EM et al., 1992). To evaluate the degree of confidence of the data obtained, images were further analyzed by the Costes randomization method using the colocalization test plugin (Costes SV et al., 2004). The Pearson's correlation coefficients were calculated between the

images of endosomes (Alexa Green Transferrin) and 25 randomized images of XY-randomized images of MitoTracker Deep Red labeled mitochondria.

2.3.6. BioRad Protein Determination Assay

Total protein concentration was determined for isolated mitochondria and endosomes, and all other collected fractions using the Bradford Protein Assay (BioRad, Hercules, CA) against a bovine serum albumin (BSA) standard curve which served as a reference for protein concentrations. The BSA and the protein samples were incubated with Bradford reagent (1:5) (BioRad, Hercules, CA) and distilled water (dH_2O) (4:5) for 5 minutes at room temperature. Optical density (OD) was read spectrophotometrically at 595 nm in disposable plastic cuvettes.

2.3.7. Immuoblot/Western Blot Analysis

The purity of isolated mitochondria, endosomes and cytosol were verified using antibodies for porin, EEA1, and eIF4e respectively. Protein expression was determined by semiquantitative immunoblots using standard methods. Thirty micrograms of protein were added to 1X SDS loading dye (62.5mM Tris pH 6.8, 2% w/v SDS, 10% glycerol, 50mM DTT, 0.01% w/v bromophenol blue) and boiled for 15 minutes. Each fraction was electrophoretically separated on a sodium dodecyl sulphate-polyacrylamide gel (SDS-PAGE). The samples were loaded in a stacking gel (4% acrylamide; 0.5M Tris-base, pH 6.8; 10% SDS; 25% ammonium persulfate APS; TEMED) and then allowed to migrate through a resolving gel (10% or 7.5% acrylamide; 1.5M Tris-base, pH 8.8; 10%SDS; 25% APS; Temed). Fractions being probed with porin and eIF4e were run on a 10%

gel whereas those being probed for EEA1 were run on 7.5% gels. Proteins migrated at 100V in 1X running buffer (25mM Tris-base; 192mM glycine; 0.1%SDS) in a BioRad electrophoresis apparatus.

Following gel migration, the samples were electrophoretically transferred to nitrocellulose membrane using transfer buffer (25mM Tris-base; 192mM glycine; 20% methanol). Membranes were then incubated overnight in 5% blocking solution (20mM Tris pH 7.5; 150mM NaCl; 0.02% Tween 20; 3% skim milk powder). Individual membranes were incubated with the respective antibody diluted in 5% blocking solution for one hour at room temperature. EEA1 antibody was diluted 1:1000, Porin 1:5000 and eIF4e 1:1000. Following incubation with primary antibody, membranes were washed 3 times for 15 minutes in TTBS (20mM Tris pH 7.5; 150mM NaCl; 0.02% Tween 20). Membranes were incubated with horseradish-peroxidase-coupled secondary antibody in a 5% milk solution for one hour at room temperature according to the following dilutions: 1:20,000 (EEA1), 1:10,000 (Porin), and 1:10,000 (eIF4e). The membranes were then washed 3 times for 15 minutes in TTBS and treated with ECL chemiluminescent substrate according to the manufacturer's instructions.

3. Results

3.1 Studies Investigating the Association of Endosomes with Mitochondria

We chose to investigate the mitochondrial and endosomal interaction using flow cytometry. Reticulocytes were double-labeled with fluorescent MitoTracker Deep Red 633 and Alexa Green Transferrin 488 specific to mitochondria and endosomes, respectively. We performed a time course in live reticuloctyes in order to examine the organellar interaction. Reticulocytes were first labeled with the mitochondrial fluorophore and following a series of wash steps, the cells were incubated at 4°C with Alexa Green Transferrin 488 for one hour in order to maximize the binding of the fluorescent tagged protein with its cell surface receptor. In contrast, endocytosis is temperature dependent, therefore once placed at 37°C, endocytosis was induced in the double-labeled reticulocytes resulting in the internalization of the fluorescent Tf and Tf-R complex. Once the double-labeled reticulocytes were placed at 37°C, endocytosis of Tf and its receptor was induced. The internalization of the fluorescent Tf permitted us to track the newly formed endosomes containing labeled Tf. Prior to flow cytometry analysis, reticuloctyes were treated with Pronase, an enzyme which non-specifically cleaves cell surface receptors. Treatment of cells with Pronase ensured that the fluorescence exhibited by flow cytometry analysis was solely due to internalized Alexa Green Transferrin bound to its cognate receptor. It needs to be emphasized that the reticulocytes were lysed prior to being subjected to flow cytometry analysis.

3.1.1. Establishment of Quadrants and Positive Controls of Fluorophores

Data obtained via flow cytometry analysis was plotted as fluorescence of MitoTracker Deep Red (MTDR) as a function of Alexa Green Transferrin fluorescence (AGTF) and was presented in logarithmic form. The dot plots were subdivided into four quadrants: upper right (UR), upper left (UL), lower right (LR) and lower left (LL) (Fig. 9). Dots located in each quadrant are referred to as "events" and represent fluorescent mitochondria, endosomes, both or non-fluorescent particles. 50,000 events in total were processed per sample and are displayed in each dot plot. The number of events found in each quadrant of a dot plot was represented as a percentage of the total number of events analyzed i.e. 50,000 events. The percentage of each quadrant is displayed in the flow cytometry dot plots.

Based on their fluorescence, events localized to specific quadrants therefore, events fluorescing both Alexa Green Transferrin and Mito Tracker Deep Red were located in the UR quadrant; events fluorescing only the mitochondrial specific fluorophore were found in the UL quadrant; events fluorescing solely Alexa Green Transferrin were displayed in the LR quadrant and non-fluorescent events collected in the LL quadrant (Fig. 9). Therefore, events located in the UL quadrant are considered single mitochondria, events in the LR quadrant represent a single endosomes and events located in the UR quadrant suggest a mitochondrial and endosomal association. Quadrant boundaries were set using the positive control of each fluorophore and the negative control devoid of

all fluorescence (Fig. 10). The positive controls were prepared by staining reticulocytes with only one fluorophore followed by lysis.

3.1.2. Endocytosis of Alexa Green Transferrin Increases with Time

As a control experiment, we performed a time course with reticulocytes labeled solely with Alexa Green Transferrin in order to ensure that the Alexa Green Transferrin was endocytosed. Reticulocytes were incubated for one hour on ice in the presence of Alexa Green Transferrin before incubating at 37°C for different time intervals. The data was once again plotted as MTDR fluorescence as a function of AGTF fluorescence. The number of events in each quadrant was represented as a percentage of the total number of events (Fig. 11). As seen in figure 11 and table 1, we noted a peak at T30' followed by a decline. We therefore concluded that endocytosis of Alexa Green Transferrin increased with time and, at approximately 30 minutes, reached a plateau.

3.1.3. Increase in the Endosomal and Mitochondria Association with Time in Double-Labeled Reticulocytes

The endosomal and mitochondrial interaction was investigated by incubating double labeled reticulocytes for different time intervals. Such an incubation yielded four populations: single endosomes located in the LR quadrant; single mitochondria located in the UL quadrant; endosomes and mitochondria located in the UR quadrant and lastly a negative population located in the LL quadrant. The number of events in each quadrant was represented as the percent of the total

number of events analyzed (Fig. 12). We noted at T0' a fluorescent population in the UR quadrant suggesting an interaction between endosomes and mitochondria prior to incubation at 37°C (Fig. 12). We determined that the latter population was in fact an autofluorescent population based on analysis of histograms and dot plots (data not shown). Because the autofluorescent population consistently represented 0.15 % of the events in the UR quadrant at each time point (data not shown), we chose not to deduct it from the percent of events in the UR quadrant at each time point.

We noted a change in the percent of all populations with respect to time (Fig. 12), however of particular importance were the populations located in the UL and UR quadrants representing mitochondria and mitochondria associated with endosomes. In order to accurately evaluate and compare the endosomal and mitochondrial association between time points, we calculated the total number of mitochondrial events located in the UR and UL quadrants for each time point presented in Figure 12. We then determined the percent of total mitochondria associated with endosomes at each time point (Fig 13). We noted an increase in the percent of total mitochondria associated with endosomes over time. The increase and the peak at T60' suggested an increasing association between endosomes and mitochondria. The decline observed may have been the result of the gradual establishment of equilibrium between the rate of endocytosis and exocytosis.

In order to examine the behaviour of the endosomal population with respect to time, we calculated the total number of endosomes using the sum of the

events of the LR and UR quadrants of Figure 12 (Table 2). Events located in the upper right quadrant represented events which emitted both the mitochondrial and endosomal fluorophore suggesting an association between endosomes and mitochondria. Events located in the LR quadrant represented events labeled solely with Alexa Green Transferrin. Therefore, the sum of the events of the two quadrants represented the total number of endosomes. Using these values, we calculated the endosomes associated with mitochondria as a percent of total endosomes at each time point. The percentages ranged between 94-98% suggesting that the majority of endosomes are associated with mitochondria at any given time. With respect to time, the percentage of total endosomes associated with mitochondria overall did not increase but remained relatively stable.

We proceeded to calculate the percent of single endosomes of total endosomes located in both the LR and UR quadrant (Table 2). The percent of single endosomes represented at most 7% of the total endosomal population. The single endosome population likely represents cytosolic endosomes in transit, i.e., shortly after endocytosis and their detachment from mitochondria.

3.1.4. Treatment of Double-Labeled Reticulocytes with Non-Fluorescent Diferric Transferrin Results in a Decrease in the Mitochondrial and Endosomal Association

In order to verify whether the population of the UR quadrant of the double label time course was the result of an association between endosomes and mitochondria, we repeated the time course, however using non-fluorescent

diferric Tf. Using T30' from the double label time course (Fig. 14A), we subdivided T30' into four samples. Each sample was incubated in the presence of 10μM of the non-fluorescent diferric Tf for an increasing amount of time at 37°C (T5, T30', T60', T120') (Fig. 14B). We predicted that incubation with the non-fluorescent diferric Tf would result in the removal of the double population from the UR quadrant and restore a single mitochondrial population. Therefore incubation of T30' at 37°C would result in the eventual exocytosis and release of fluorescent Tf in exchange for non-fluorescent diferric Tf present in the incubation media. The experiment presented in Fig. 14A basically repeated the experiment shown in Fig. 12 (Please note that the percent of the double-labeled population [UR quadrant] was much higher than in the experiment presented in Fig. 12; this was caused by a much larger content of reticulocytes in this sample [Fig. 7]). In Figure 14 A and B, the number of events found in each quadrant was represented as a percentage of the total number of events analyzed.

During the second incubation, the treatment of double-labeled reticulocytes with unlabeled diferric Tf resulted in a decrease in the percentage of the double-labeled population (UR quadrant) (Fig. 14B). We noted the same trend when we determined the percentage of total mitochondria associated with endosomes before and during the treatment with non-fluorescent differic Tf (Fig. 15). We, therefore, conclude that the double population is composed of endosomes associated with mitochondria. Furthermore, the gradual dissociation of the mitochondrial and endosomal association suggests that the interaction between the two organelles is reversible and specific (Fig. 15). Interestingly, the treatment

failed to completely remove the double population and restore a single mitochondrial population indicating that some fluorescent Alexa Green Transferrin remained within the cell and was not exocytosed. This result suggests that reticulocytes can never be completely devoid of Tf, therefore, at any given point in time, a baseline level of Tf exists within the cell.

3.1.5. Inhibitors, Bafilomycin and W-7, Reduce Mitochondrial and Endosomal Association

We next proceeded to determine whether the interaction could be inhibited by employing agents that block iron release from Tf or interfere with the endocytic pathway. Bafilomycin inhibits acidification of the endosomes (Finbow et al., 1997; Zhang et al., 2005) and W-7, a myosin light chain kinase inhibitor (Ito et al., 1989; Bourguinon et al., 1998), blocks endocytosis and intracellular endosomal motility (Sheftel et al., 2007). Firstly, reticulocytes were incubated with MTDR, washed and then incubated for 1 hour with AGTF at 4°C. Following the 1 hour incubation, the inhibitor was added to the reticulocyte suspension and incubated for 30 minutes at 4°C. The reticulocyte suspension was then added to pre-warmed media containing 2.5 μM of AGTF and incubated for 30 minutes at 37°C. The control was subjected to the above mentioned incubation periods both at 4°C and 37°C in the absence of an inhibitor. In order to test the toxicity of the solvents, additional samples were added using only the volume of the vehicle alone. Each respective solvent was added to reticulocytes at the same volume as the maximum concentration used for its specific drug. In Figures 16 and 18, the

number of events found in each quadrant was represented as the percentage of the total number of events analyzed.

With increasing concentrations of bafilomycin, we noted a decrease in the percent of the double population (Fig. 16). We further evaluated the effect of bafilomycin on the mitochondrial and endosomal association by calculating the percentage of total mitochondria associated with endosomes for each concentration. As previously described, we determined the total number of mitochondria by adding the total number of events located in the UL and UR quadrants which represented single mitochondria and mitochondria associated with endosomes respectively. We noted a decrease in the percentage of total mitochondria associated with endosomes with increasing concentrations of bafilomycin in comparison with the control (Fig. 17). The solvent control (DMSO) resulted in an increase in the percentage of total mitochondria associated with endosomes which in fact exceed the percentage of the control. Together these results confirm that the decrease in the percentage of the total mitochondria associated with endosomes was the result of the inhibitor itself and not the solvent.

Treatment of reticulocytes with W-7 resulted in a decrease in the double population in comparison with the control (Fig. 18). Once again, we calculated the percentage of the total mitochondria associated with endosomes and noted a decrease in the percentage of total mitochondria associated with endosomes with increasing concentrations of W-7 in comparison with the control (Fig. 19). Treatment of the reticulocytes with the solvent, methanol, resulted in a decrease in

the percentage of the total mitochondria associated with endosomes; however, the decrease was less than that seen when the maximum concentration of W-7 was added.

Overall, we found that the employment of inhibitors reduced the association between mitochondria and endosomes. Together these findings suggest that the association between endosomes and mitochondria is specific.

3.2 Cell-Free Assays

3.2.1. Erythroid Cell-Free Assay

3.2.1.1. Isolation of Mitochondria and Endosomes from Erythroid Cells

We successfully isolated mitochondria from erythroblasts and early endosomes from reticulocytes. We chose not to isolate mitochondria from reticulocytes because reticulocytes likely contain less mitochondria than erythroblasts; therefore, we chose to isolate mitochondria from splenic erythroblasts. In order to verify whether we had successfully isolated mitochondria and endosomes, we used Anti-Porin and Anti-EEA1, antibodies specific to mitochondrial and endosomal proteins, respectively (Fig. 20A). We also verified contamination of each organellar fraction with cytosol using the cytosolic translation initiation factor eIF4e (Fig. 20B). We noted slight cytosolic contamination within our organellar fraction of both endosomes and mitochondria. Contamination is inevitable when isolating organelles via differential centrifugation moreover the presence of eIF4e in the organellar fractions was observably less than its presence in the cytosol of each organelle.

3.2.1.2. Endosomes and Mitochondria colocalize in Erythroid Cell-Free Assay

In order to further confirm the interaction between endosomes and mitochondria suggested by flow cytometry, we established a cell-free assay using isolated fluorescent endosomes and mitochondria (Fig. 21). The assay consisted of the fluorescent organelles, ATP, GTP, fusion buffer (FB) and reticulocyte derived cytosol.

The colocalization of endosomes and mitochondria was first evaluated qualitatively by overlaying the red and green images. The merge image showed a number of regions where the two signals appeared to colocalize. In order to evaluate the colocalization quantitatively, the Pearson's correlation coefficient (Rr) was calculated for four different data sets. A Rr value of 0 indicates no correlation and therefore no colocalization. A Rr value of 1 indicates a perfect correlation and therefore colocalization, and lastly, values less than 0.5 are regarded as inconclusive. The four data sets used produced Rr values which ranged from 0.148 to 0.249 and therefore nothing could be concluded regarding the colocalization of endosomes and mitochondria. In order to verify the Rr values attained, we performed the Costes randomization test. The pixels in the mitochondria images were randomized. The Pearsons' correlation coefficient between the endosome image and the randomized mitochondria image was calculated. The randomization process and correlation was repeated 25 times. The Pearsons' correlation coefficients obtained following randomizations were compared with the original observed non-randomized correlation coefficient,

R(obs) (Table 3). In all four data sets (a, d, e and f), the correlation coefficients following randomization, R(rand), were close to zero. The p-value was calculated between R(rand) and the R(obs) data sets and was 0.99 which indicated that there was no correlation between the randomized and observed data sets. Although the R(obs) values were low and were thus inconclusive, the R(rand) values were virtually zero. The p-value of 0.99 indicated that the two data sets were not correlated and there is a strong degree of confidence that the initially observed Rr (obs) values (0.148 to 0.249) did not occur by chance (Table 3). Therefore, we concluded that the colocalization seen in the erythroid assay was not random, and strongly suggests that the mitochondria and endosomes were indeed in contact.

3.2.2. HeLa Cell-Free Assay

We then proceeded to test whether the endosomal mitochondrial interaction seen in the erythroid cell-free assay was dependent on the mitochondria being functional. We repeated the cell-free assay using YFP-tagged fluorescent mitochondria isolated from HeLa cells with the addition of the mitochondrial uncoupler, CCCP (Fig. 22). We did not repeat the erythroid assay in the presence of the uncoupler because the mitochondrial dye, MitoTracker Deep Red is only retained by respiring mitochondria. Therefore, the addition of CCCP would only result in the dissipation of the fluorescent dye.

We determined the percent of total mitochondria colocalizes with endosomes in assays treated with or without the uncoupler. We counted 200 mitochondria in each assay and repeated the experiment three times. In

comparison with the control, we noted a statistically significant decrease ($p < 0.0153$) in the percent of total mitochondria associated with endosomes (Fig. 23). This result indicates that the interaction between the two organelles requires that the mitochondria be metabolically active. The result also confirms that the interaction occurring between the two organelles is specific and not the result of non-specific binding.

4. Discussion

4.1 Flow Cytometry Studies

The purpose of our flow cytometry studies was to demonstrate the endosomal-mitochondrial interaction. Time course experiments involving reticulocytes, labeled with both mitochondrial and endosomal fluorophores, suggested an interaction between the organelles that was both specific and reversible. Cells were lysed and were centrifuged in order to remove cellular debris and the supernatant subjected to cytometry analysis. For each sample, 50,000 events were processed; these events were comprised of fluorescently labeled mitochondria, endosomes or non-fluorescently labeled intracellular structures.

We chose to examine the mitochondrial population and its association with endosomes with respect to time. Therefore, data was presented as the percentage of total mitochondria associated with endosomes. We chose this means of analysis due to the variation of the total number of mitochondria between time points. We applied this analysis to all time courses performed with the exception of the single labeled Alexa Green Transferrin time course.

4.1.1. Time course of Double-Labeled Reticulocytes

In the time course of double-labeled reticulocytes, we noted an increase in the percentage of total mitochondria associated with endosomes which peaked at T60', following this time interval there was virtually no change (Fig. 13). The maximum percentage attained was 25% suggesting that approximately 75% of total mitochondria did not associate with endosomes (Fig. 13). Given the

efficiency with which immature erythrocytes acquire and incorporate iron into heme this finding is not surprising. As already discussed, heme synthesis in immature erythroid cells occur at an astonishing rate, on a per-cell basis the rate of heme synthesis is at least one order of magnitude higher than in the liver, the second highest heme producer in the organism (Ponka, 1997). Therefore, in agreement with this unique quality of heme biosynthesis in immature erythroid cells, an excess of mitochondria within the cell would ensure that heme biosynthesis is not limited. It could be possibly argued that non-fluorescently labeled endosomes were formed during the incubation at 37°C, and thus endosomal-mitochondrial associations would not have been detected by flow cytometry. We believe this scenario to be unlikely because reticulocytes were incubated in media which was not supplemented with nutrients and contained only fluorescent iron-bound Tf.

The increase in the percentage of the total mitochondria associated with endosomes was attributed to increasing endocytosis of Alexa Green Transferrin. This conclusion is supported by the time course performed using reticulocytes labeled solely with Alexa Green Transferrin (Fig.11). Because our findings suggest that the mitochondria are in excess, the peak at T60' reflects the gradual establishment of equilibrium between the rate of endocytosis and exocytosis (Fig. 13). Interestingly, we noted that the percentage of endosomes associated with mitochondria was at least 94% of total endosomes available meaning that at any given time, the majority of endosomes are associated with mitochondria. These findings are not surprising considering that the primary function of reticulocytes is

to acquire iron for the synthesis of hemoglobin. In experiments conducted with reticulocytes labeled with both Alexa Green Transferrin and FM1-43, a plasma membrane specific dye, it was noted that when the dual labeled reticulocytes were incubated in the presence of full media (containing 10% fetal calf serum), all of the endocytic vesicles labeled with Alexa Green Transferrin colocalized with FM-143 (Sheftel, Zhang et al. 2007). Therefore, the vast majority of the reticulocyte's endocytic machinery is occupied by Tf and reserved for iron trafficking.

4.2. Endosomal Involvement in Iron Delivery to the Mitochondria

Using inhibitors of endosomal acidification and motility, bafilomycin and W-7 respectively, the percent of total mitochondria associated with endosomes was decreased in comparison with the control. Although inhibition by W-7 was moderate, our findings are in agreement with recently published data. Live confocal microscopy studies using reticulocytes stained with a specific mitochondrial dye, treated with W-7 and subsequently incubated with Alexa Green Transferrin resulted in the inhibition of endocytosis of the fluorescent Tf (Sheftel, Zhang et al. 2007). Additionally, incubation of the reticulocytes with Alexa Green Transferrin, followed by treatment with W-7, resulted in the immobilization of the fluorescently labeled Tf containing endosomes. In order to determine whether this immobilization of endosomes would inhibit delivery of iron to the mitochondria, the investigators repeated the experiment, but using ^{59}Fe. Treatment of reticulocytes with W-7 resulted in an inhibition of ^{59}Fe incorporation

into heme. Together these earlier findings and those reported here confirm that endosomal motility facilitates iron incorporation into heme.

Endosomal involvement has been further confirmed by the recent discovery of the genetic mutation in the haemoglobin deficit (*hbd*) mouse (Lim, Jin et al. 2005; White, Boydston et al. 2005) resulting in reduced Tf cycling (Zhang, Sheftel et al. 2006). The *hbd* mouse is characterized by hyprochromic, microcytic anemia that is inherited in an autosomal, recessive manner. The defect was identified as an exon deletion in Sec1511, the mammalian homologue of a yeast gene which encodes a protein involved in the exocytic pathway. Interestingly, the yeast homologue encodes a key protein involved in vesicle docking (White, Boydston et al. 2005). We postulate that this protein may be implicated in the transient associations between mitochondria and endosomes in reticulocytes revealed by live-imaging confocal microscopy (Sheftel, Zhang et al. 2007), lending further support to our hypothesis that a direct interaction between the organelles facilitates iron transfer.

4.3. Mitochondrial and Endosomal Association

Over twenty years ago, using electron microscopy examination, Isobe et al. (1981) reported that cytoplasmic Tf was found not only in "micropinocytotic" vesicles but also on the mitochondrial membrane of immature erythroid cells. This study provided preliminary evidence of the association between the two organelles and was in agreement with a proposal made earlier suggesting that a direct interaction between endosomses and mitochondria may be required for the

transfer of iron (Ponk, Neuwirt et al. 1976). The results obtained from our confocal microscopy cell-free assays have provided further support and evidence for this intimate association between the two organelles. It was demonstrated in the erythroid cell-free assay that the mitochondria and endosomes colocalized (Fig. 21). Using HeLa cells, we noted an association between the organelles that could be disrupted with a mitochondrial uncoupler, CCCP (Fig. 22). These results indicate that the association between the organelles was in fact specific and more importantly, suggested that the association required actively respiring mitochondria. In order to reach ferrochelatase, iron must traverse both the outer and inner mitochondrial membrane, therefore we postulate that the transfer of iron requires the membrane potential of the mitochondria.

4.4. Labile Iron Pool

The recent publications produced by our laboratory and the findings presented in my work together strongly undermine the existence of the LIP in erythroid cells. It is widely accepted that, upon its exit from the endosome, iron enters a cytosolic intermediate pool comprised of low molecular weight (M_r) iron intermediates, which act as a source of iron for intracellular sites of utilization (Jacobs, 1977). This elusive intermediate has never been identified.

One study closely examined the intermediates of iron metabolism in reticulocytes treated in the presence and absence of succinylacetone (SA), an inhibitor of heme synthesis which resulted in the accumulation of iron in the mitochondria (Richardson et al. 1996). These investigators examined the

distribution of ^{59}Fe in low and high M_r molecules in control and SA-treated reticulocytes. They found that a small amount of ^{59}Fe was present in a low-M_r form in the cytosol of control or SA-treated reticulocytes, with most iron being incorporated into the mitochondrial fraction and high-M_r molecules. Interestingly, when heme synthesis was inhibited with SA, the amount of ^{59}Fe in the low-M_r compartment was significantly less than in the control reticulocytes. It was suggested that the low-M_r component might either be heme or a low molecular weight component containing heme. The investigators argued that if in fact the iron within the low-M_r compartment served as an intermediate for heme synthesis, uptake of ^{59}Fe into the compartment should increase and plateau early on during the ^{59}Fe incubation however, this was not the case. When incubating reticulocytes with ^{59}Fe and measuring the ratio between ^{59}Fe incorporation into heme and the total cell-associated ^{59}Fe, an equilibrium was attained within five minutes of reticulocyte incubation with ^{59}Fe. Therefore, a steady-state should also have been attained in the intermediate low-M_r compartment, instead ^{59}Fe uptake increased linearly as a function of incubation time. Therefore the kinetic behaviour of the iron in the low-M_r compartment is contrary to the behaviour of an expected iron-intermediate. These findings make the idea of a cytosolic intermediate pool composed of low-M_r iron intermediates that serve as a source of iron for hemoglobin synthesis highly unlikely.

In the current literature, studies seeking to elucidate the LIP have employed chelators in order to estimate the iron concentration of the LIP; the most commonly used compound is fluorescent. It has been shown that when cells

are loaded with calcein and incubated with diferric Tf, the chelator is capable of intercepting iron from the endosomes when cells are metabolically active (Breuer et al. 1995). It is not surprising that calcein is capable of intercepting iron following its release from endosomes when the cells are metabolically active. Zhang et al (2005) have shown that when membrane permeable chelators are added to reticulocytes at 4°C following a 45 minute incubation with ^{59}Fe, less than 5% of the total cell-associated iron is chelated. On the contrary, when chelators were added during the 45 minute incubation with ^{59}Fe at 37°C , 70% of the total cell-associated iron was chelated. Therefore, when the cell is metabolically active, iron is released from Tf within the endosome and eventually is inserted into ferrochelatase by protoporphyrin IX. Following its release from Tf and prior to its insertion into protoporphyrin IX, iron is susceptible to chelation. Cabantchik and colleagues (Breuer et al. 1995; Cabantchik et al. 2008), consider this chelatable iron equivalent to the cytosolic LIP, when in fact it represents iron that has been captured while in transit from one ligand to the next. Therefore, when iron is released from Tf within the endosome and prior to its insertion into protoporphyrin IX, it is susceptible to being chelated by calcein. Therefore, chelation of iron by calcein may in fact represent iron that has been stripped from organelles i.e. endosomes and mitochondria, during its active transfer and not iron that has been removed from the LIP.

A recent publication produced by our lab has demonstrated that endosomal iron in reticulocytes completely bypasses the cytosol which further undermines the existence of a low-M_r iron intermediate (Sheftel, Zhang et al. 2007). In this

study, reticulocytes were loaded with a membrane impermeable chelator and incubated with $^{59}Fe_2$-Tf. The presence of the cytosolic chelator did not inhibit incorporation of ^{59}Fe into heme which means that Tf-borne ^{59}Fe bypasses the cytosol.

In light of recent publications produced by our laboratory and the results reported here, the existence of a freely diffusible iron pool in the cytosol is unlikely. Due to the potential toxicity of iron and the incredible efficiency of its incorporation into heme in erythroid cells, a more attractive model of iron transfer within reticulocytes is the one that requires a transient association between endosomes and mitochondria.

4.5 Future Directions

Since it was first proposed over twenty years ago, much has been learnt regarding the endosomal and mitochondrial association in erythroid cells. In this study, we have provided evidence of a physical interaction between the organelles. In order to further elucidate the association between endosomes and mitochondria, the use of agents capable of inhibiting the association may provide novel information regarding the interaction. Lysosomotropic agents such as ammonium chloride (NH_4Cl) and chloroquinine have been shown to inhibit iron uptake in reticulocytes without causing a decrease in Tf endocytosis therefore further investigation is required in order to determine the cause of inhibition (Iacopetta and Morgan, 1983). The endosomal and mitochondrial association should also be investigated via immunoblot analysis in order to determine whether endosomal

markers such as EEA1 and Tf-R are present in the mitochondrial fraction isolated from reticulocytes. Lastly, proteomic analysis of isolated endosomes and mitochondria-endosomal complexes might be useful to identify proteins perhaps involved with the mitochondrial and endosomal association.

5. References

Andrews, N. C. (2002). "A genetic view of iron homeostasis." Semin Hematol **39**(4): 227-34.

Aslan, D., K. Crain, et al. (2007). "A new case of human atransferrinemia with a previously undescribed mutation in the transferrin gene." Acta Haematol **118**(4): 244-7.

Borova, J., P. Ponka, et al. (1973). "Study of intracellular iron distribution in rabbit reticulocytes with normal and inhibited heme synthesis." Biochim Biophys Acta **320**(1): 143-56.

Bourguignon, L.Y., Z. Gunja-Smith, et al.(1998). "CD44v(3.8-10) is involved in cytoskeleton-mediated tumor cell migration and matrix metalloproteinase (MMP-9) association in metastatic breast cancer cells." J Cell Physiol **176** (1):206-215.

Breuer, W., S. Epsztejn, et al. (1995). "Iron acquired from transferrin by K562 cells is delivered into a cytoplasmic pool of chelatable iron (II)." J Biological Chemistry **270**(41): 24209-215.

Cabantchik, Z.I., W. Breuer, et al. (2008). "Intracellular Labile Iron." Int J Biochem Cell Biol **40**(3): 350-4.

Chan, R. Y., C. Seiser, et al. (1994). "Regulation of transferrin receptor mRNA expression. Distinct regulatory features in erythroid cells." Eur J Biochem **220**(3): 683-92.

Costes S.V., Daelemans D., et al. (2004). "Automatic and quantitative measurment of protein-protein colocalization in live cells." Biophys Journal **86** (6): 3993-4003.

Fenton, H. J. H. "On a new reaction of tartaric acid." Chemical News **33** (1876): 190.

Finbow, M., M.A. Harrison (1997)"The vacuolar H+-ATPase: a universal proton pump of eukaryotes."Biochem J **324** (3): 697-712.

Ganz, T. and E. Nemeth (2006). "Regulation of iron acquisition and iron distribution in mammals." Biochim Biophys Acta **1763**(7): 690-9.

Greenough, W. B., 3rd, T. Peters, Jr., et al. (1962). "An intracellular protein intermediate for hemoglobin formation." J Clin Invest **41**: 1116-24.

Gunshin, H., B. Mackenzie, et al. (1997). "Cloning and characterization of a mammalian proton-coupled metal-ion transporter." Nature **388**(6641): 482-8.

Halliwell, B. and J. M. Gutteridge (1990). "Role of free radicals and catalytic metal ions in human disease: an overview." Methods Enzymol **186**: 1-85.

Harrison, P. M. and P. Arosio (1996). "The ferritins: molecular properties, iron storage function and cellular regulation." Biochim Biophys Acta **1275**(3): 161-203.

Iacopetta, B.J., E.H. Morgan. (1983). "The kinetics of transferrin endocytosis and iron uptake from transferrin in rabbit reticulocytes." J Biol Chem **258**(15): 9108-115.

Isobe, K., Y. Isobe et al. (1981). "Cytochemical demonstration of transferrin in the mitochondria of immature human erythroid cells." Acta Haematol **65**: 2-9.

Ito, M., F. Tanabe et al. (1989). "Possible involvement of microfilaments in protein kinase C translocation." Biochem Biophys Res Commun **160** (3): 1344-1399.

Jacobs, A. (1977). "Low molecular weight intracellular iron transport compounds." Blood **50**(3): 433-9.

Knutson, M. and M. Wessling-Resnick (2003). "Iron metabolism in the reticuloendothelial system." Crit Rev Biochem Mol Biol **38**(1): 61-88.

Kuhn, L. C. (1994). "Molecular regulation of iron proteins." Baillieres Clin Haematol **7**(4): 763-85.

Laskey, J. D., P. Ponka, et al. (1986). "Control of heme synthesis during Friend cell differentiation: role of iron and transferrin." J Cell Physiol **129**(2): 185-92.

Levy, J. E., O. Jin, et al. (1999). "Transferrin receptor is necessary for development of erythrocytes and the nervous system." Nat Genet **21**(4): 396-9.

Lim, J.E. , O. Jin, et al. (2005). "A mutation in Sec1511 causes anemia in hemoglobin deficit (hbd) mice." Nat Genet **37**: 1270-1273.

Manders E.M., Stap J., et al. (1992). " Dynamics of three-dimensional replication patterns during the S-phase, analysed by double labelling of DNA and confocal microscopy." Journal of Cell Science **103** (3):857-862.

Martinez-Medellin, J. and H. M. Schulman (1972). "The kinetics of iron and transferrin incorporation into rabbit erythroid cells and the nature of stromal-bound iron." Biochim Biophys Acta **264**(2): 272-4.

McLintock, L. A. and E. J. Fitzsimons (2002). "Erythroblast iron metabolism in sideroblastic and sideropenic states." Hematology **7**(3): 189-95.

Napier, I., P. Ponka, et al. (2005). "Iron trafficking in the mitochondrion: novel pathways revealed by disease." Blood **105**(5): 1867-74.

Ohgami, R. S., D. R. Campagna, et al. (2005). "Identification of a ferrireductase required for efficient transferrin-dependent iron uptake in erythroid cells." Nat Genet **37**(11): 1264-9.

Pollycove, M. (1964) "Iron Kinetics." In: Gross, F. (ed.). Iron Metabolism: An international symposium. (148-177). Berlin: Springer-Verlag.

Ponka, P., J. Neuwirt, et al. (1976). "Control of iron delivery to hemoglobin in erythroid cells." Ciba Foundation Symposium. 167-200.

Ponka, P., A. Wilczynska, et al. (1982). "Iron utilization in rabbit reticulocytes. A study using succinylacetone as an inhibitor or heme synthesis." Biochim Biophys Acta **720**(1): 96-105.

Ponka, P. and H.M. Schulman (1985). "Acquisition of iron from transferrin regulates reticulocyte heme synthesis." J Biol Chem **260**(27): 14717-21.

Ponka, P. (1997). "Tissue-specific regulation of iron metabolism and heme synthesis: distinct control mechanisms in erythroid cells." Blood **89**(1): 1-25.

Ponka, P. (1999). "Cell biology of heme." Am J Med Sci **318**(4): 241-56.

Ponka, P.(2002). "Iron Utilization in Erythrocyte Formation and Hemoglobin Synthesis." In Templeton, D.M.(Eds.) Molecular and Cellular Iron Transport. (643-677). Toronto, Ontario: Marcel Dekker.

Ponka, P., A. D. Sheftel, et al. (2002). "Iron targeting to mitochondria in erythroid cells." Biochem Soc Trans **30**(4): 735-8.

Ponka, P. (2003) "Recent Advances in Cellular Iron Metabolism." The Journal of Trace Elements **16**:201-217.

Primosigh, J. V. and E. D. Thomas (1968). "Studies on the partition of iron in bone marrow cells." J Clin Invest **47**(7): 1473-82.

Rasband, W.S., National Institutes of Health, Bethesda, Maryland, USA, http://rsb.info.nih.gov/ij/, 1997-2004

Richardson, D. R., P. Ponka, et al. (1996). "Distribution of iron in reticulocytes after inhibition of heme synthesis with succinylacetone: examination of the intermediates involved in iron metabolism." Blood **87**(8): 3477-88.

Richardson, D. R. and P. Ponka (1997). "The molecular mechanisms of the metabolism and transport of iron in normal and neoplastic cells." Biochim Biophys Acta **1331**(1): 1-40.

Schalinske, K.L., S.A. Anderson, et al. (1997). "The iron-sulfur cluster of iro regulatory protein I modulates the accessibility of RNA binding and phosphorylation sites." Biochemistry **36**: 3950-3958.

Scott, M. D. and J. W. Eaton (1995). "Thalassaemic erythrocytes: cellular suicide arising from iron and glutathione-dependent oxidation reactions?" Br J Haematol **91**(4): 811-9.

Shaw, G.C., J.J. Cope, et al. (2006). "Mitoferrin is essential for erythroid iron assimilation" Nature **440**(2): 96-100.

Sheftel, A. D. (2006). "The Handling of Iron by Erythroid and Erythrophagocytic Cells." Ph. D Thesis. McGill University. pg. 30.

Sheftel, A. D., A. S. Zhang, et al. (2007). "Direct interorganellar transfer of iron from endosome to mitochondrion." Blood **110**(1): 125-32.

Theil, E. C., R. A. McKenzie, et al. (1994). "Structure and function of IREs, the noncoding mRNA sequences regulating synthesis of ferritin, transferrin receptor and (erythroid) 5-aminolevulinate synthase." Adv Exp Med Biol **356**: 111-8.

Trenor, C. C., 3rd, D. R. Campagna, et al. (2000). "The molecular defect in hypotransferrinemic mice." Blood **96**(3): 1113-8.

White, R.A., L.A. Boydston, et al. (2005). "Iron metabolism mutant hbd mice have a deletion in Sec1511, which has homology to a yeast gene for vesicle docking." Genomics **86**:668-673.

Wintrobe, M.M. (1995). "Wintrobe's Clinical Hematology." In: Greer JP et al., (Eds.) (113-22). Philadelphia, PA: Lippincott Williams and Wilkins Inc.

Zail, S. S., R. W. Charlton, et al. (1964). "Studies on the Formation of Ferritin in Red Cell Precursors." J Clin Invest **43**: 670-80.

Zhang, A. S., A. D. Sheftel, et al. (2005). "Intracellular kinetics of iron in reticulocytes: evidence for endosome involvement in iron targeting to mitochondria." Blood **105**(1): 368-75.

Zhang, A.S., A.D. Sheftel, et al. (2006). "The anemia of "haemoglobin-deficit" (hbd/hbd) mice is caused by a defect in transferrin cycling." Experimental Hematology **34** (5): 593-598.

Table 1. Increase in the Percent of Total Number of Events Located in the Endosomal Population (LR quadrant)

Time (min)	T0'	T1'	T5'	T15'	T30'	T60'
Endosomes (Lower Right Quadrant)	0.09	0.48	0.97	1.73	2.45	2.15

Table 2. Majority of Total Number of Endosomes are Associated with Mitochondria

Time (min)	Number of Endosomes Associated with Mitochondria (UR Quadrant)	Number of Single Endosomes (LR Quadrant)	Total Number of Endosomes (UR+LR)	Single Endosomes as a Percent of Total Endosomes (%)	Endosomes Associated with Mitochondria as a Percent of Total Endosomes (%)
T0'	1534	5	1539	-	-
T1'	3409	86	3495	2.52	97.54
T5'	8859	505	9364	5.70	94.61
T15'	17159	343	17502	2.00	98.04
T30'	18606	1172	19778	6.30	94.07
T60'	17584	777	18361	4.42	95.77
T90'	16184	617	16801	3.81	96.33

* The numbers at T0' in the UR and LR quadrants represent the autofluorescent population previously mentioned in the results.

Table 3. Statistical Analysis of Erythroid Cell-Free Assay Demonstrates that Colocalization Does Not Occur by Chance

Image	Rr(obs)	R(rand) mean±sd	P-value	Trials
Endo 1 and Mito 1	0.148	-0.010±0.002	0.9	25
Endo 2 and Mito 2	0.193	-0.001±0.002	0.9	25
Endo 3 and Mito 3	0.171	-0.001±0.002	0.9	25
Endo 4 and Mito 4	0.249	-0.002±0.002	0.9	25

The Pearson correlation coefficient was determined for four data sets of mitochondria and endosomes [Rr(obs)]. Following randomization of the mitochondrial image the Pearson correlation coefficient was determined between the endosome image and the corresponding mitochondria image [R(rand)]. The p-value of 0.9 indicated that there was no correlation between the Rr(obs) and R(rand) for each data set emphasizing that the colocalization did not occur by chance.

sd: Standard Deviation

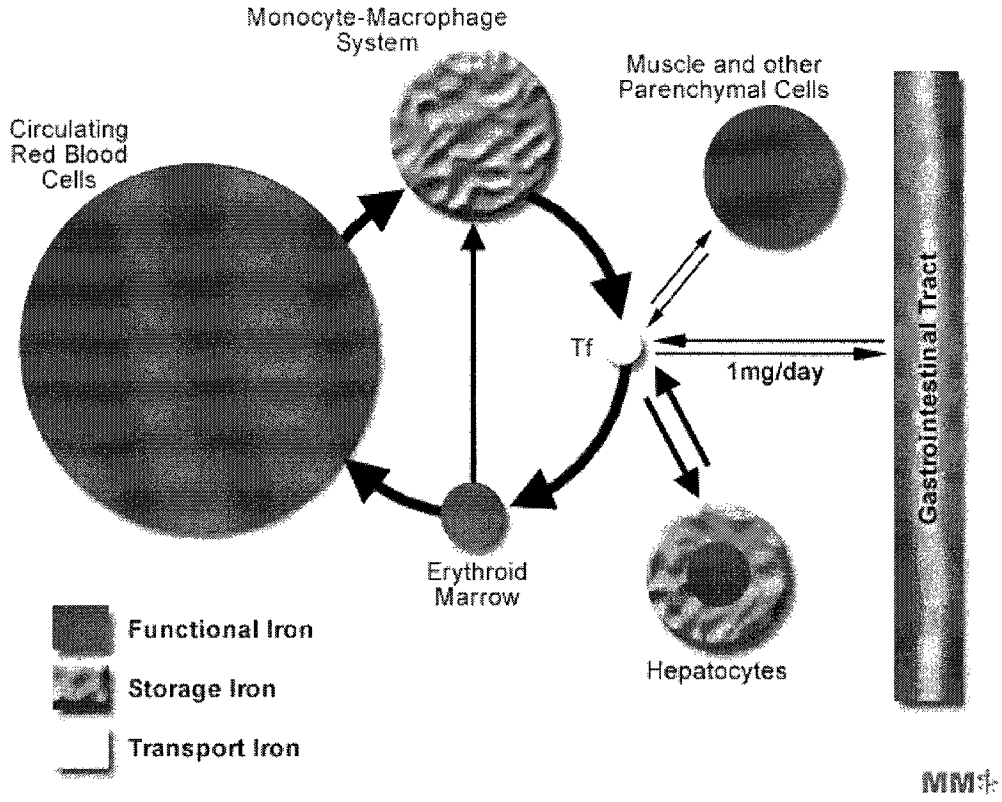

Figure 1. Mammalian Iron Cycle

The figure represents the routes of iron movement within the adult. The area of each circle is proportional to the amount of iron contained in the compartment and the width of each arrow is proportional to the daily flow of iron from one compartment to another. Transferrin (Tf), the plasma glycoprotein, transports iron between sites of storage and utilization.
(Adapted from Pollycove, 1964)

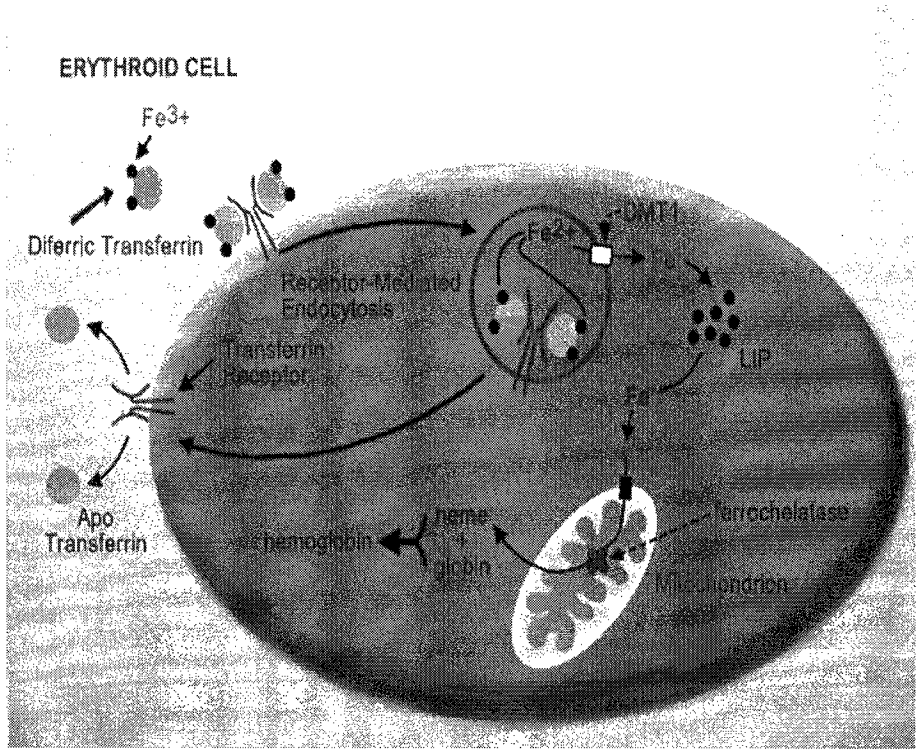

Figure 2. Acquisition and Incorporation of Iron into Heme by Erythroid Cells

Firstly, diferric transferrin binds to the transferrin receptor located on the cell surface. Following endocytosis, the iron is released from transferrin via acidification of the endosome via a proton pump. It is then reduced by a ferric reductase and expelled from the endosome via the divalent metal transporter 1 (DMT1). Iron is then believed to equilibrate with a low molecular weight labile iron pool (LIP). Eventually, iron will make its way to the mitochondria, the site of heme biosynthesis. Once complexed with iron, heme is exported from the mitochondria where it will be combined with globin in the cytosol to form hemoglobin.
(Ponka)

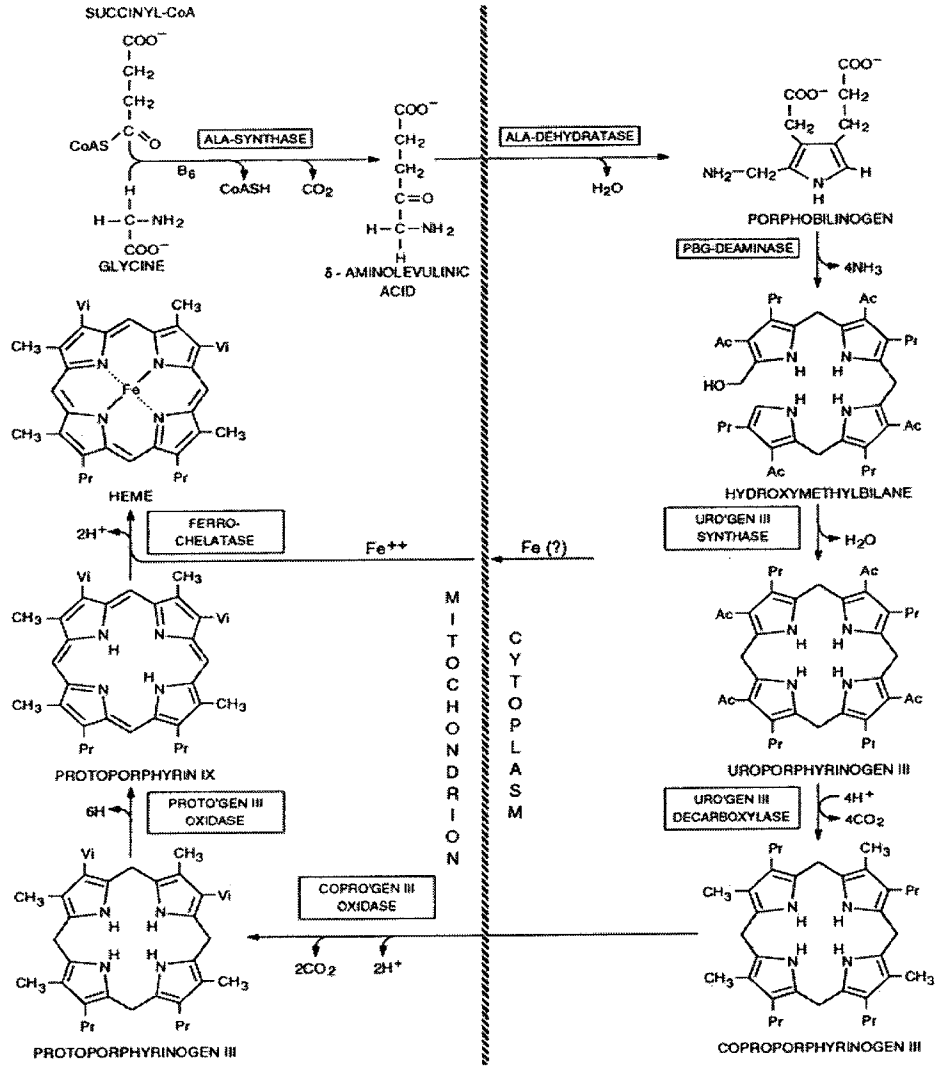

Figure 3. The Heme Biosynthetic Pathway

The heme biosynthesis pathway consists of eight enzymes, evenly divided between the mitochondria and cytosol. The fist step, the formation of aminolevulinic acid (ALA), occurs in the mitochondria. The following four steps, including the synthesis of coproporphyrinogen III, occur in the cytoplasm. The final three steps take place in the mitochondria and end with the insertion of ferrous iron (Fe^{2+}) into the protoporphyrin IX ring.
(Ponka, 1999)

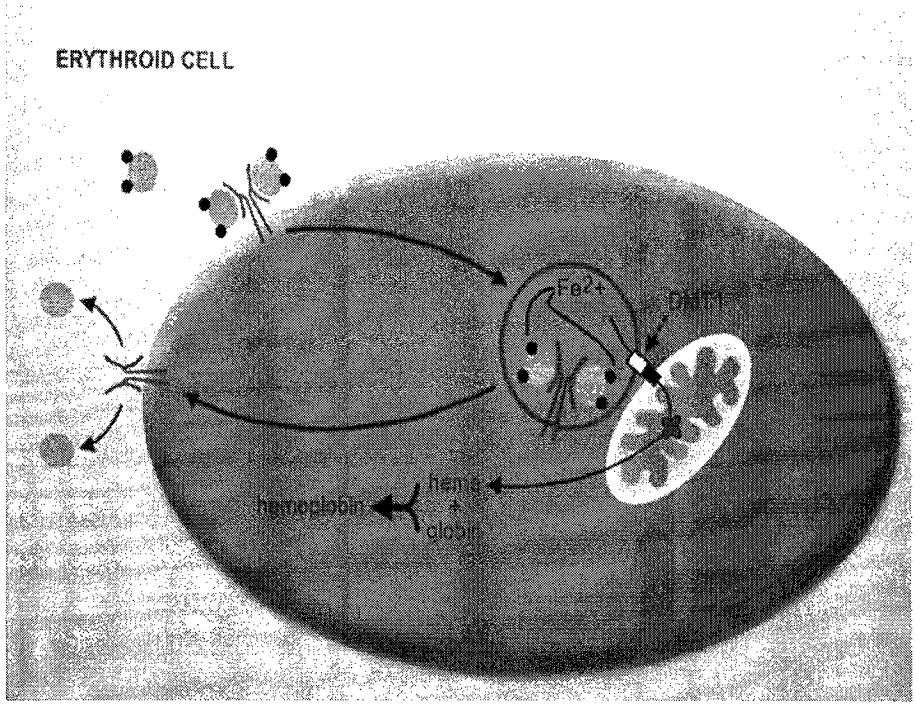

Figure 4. Transfer of Iron May Require the Direct Interaction between Iron Laden Endosomes and Mitochondria

The more recent model of intracellular iron transport within erythroid cells suggests that iron is delivered from endosomes directly to the mitochondria, completely bypassing the cytosol. More precisely, iron is handed directly from endosomal protein to mitochondrial protein and remains protein-bound until it reaches ferrochelatase in the mitochondria, its final point of destination.
(Ponka)

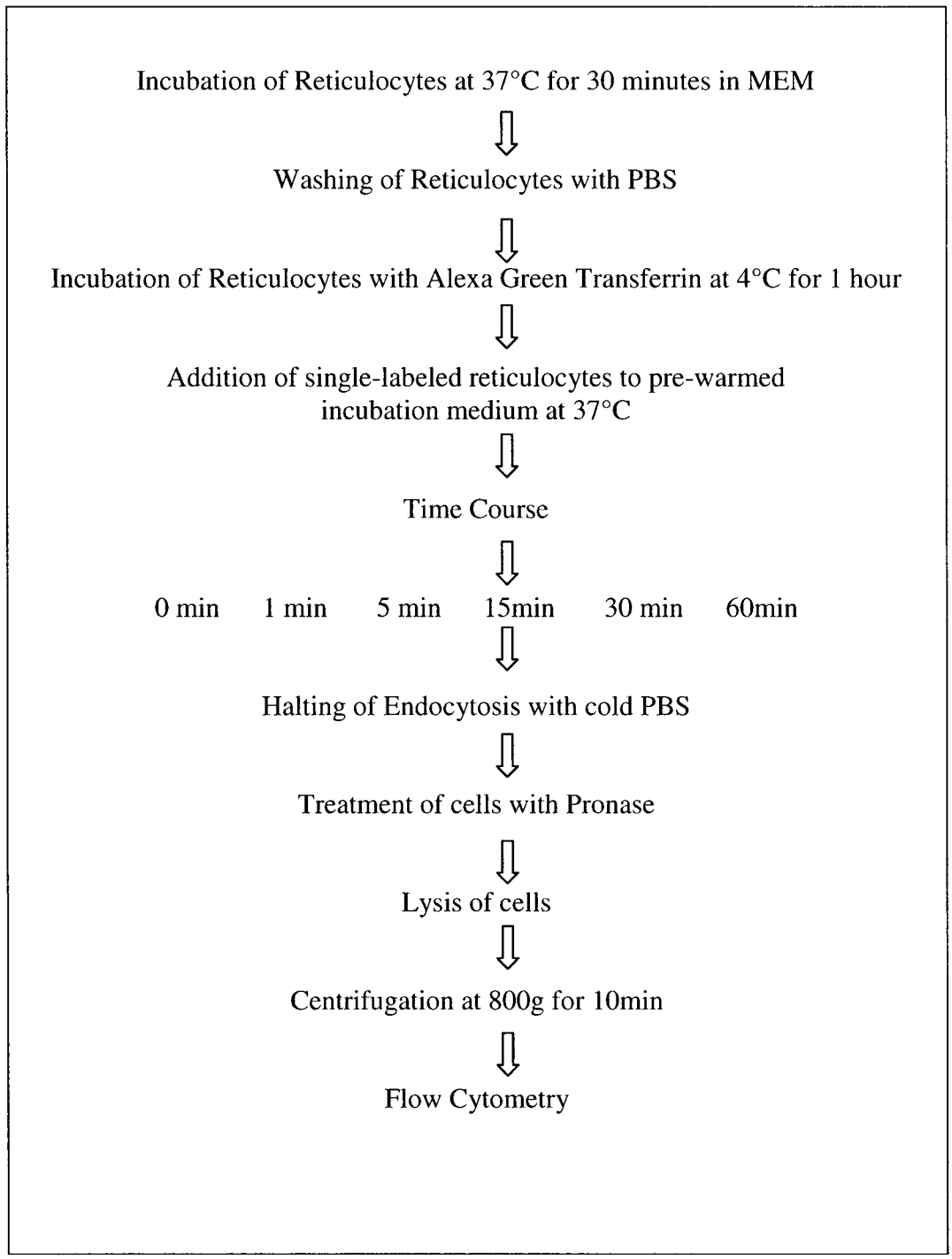

Figure 5 –Time Course of Alexa Green Transferrin Labeled Reticulocytes
Protocol for staining reticulocytes with Alexa Green Transferrin and for time course

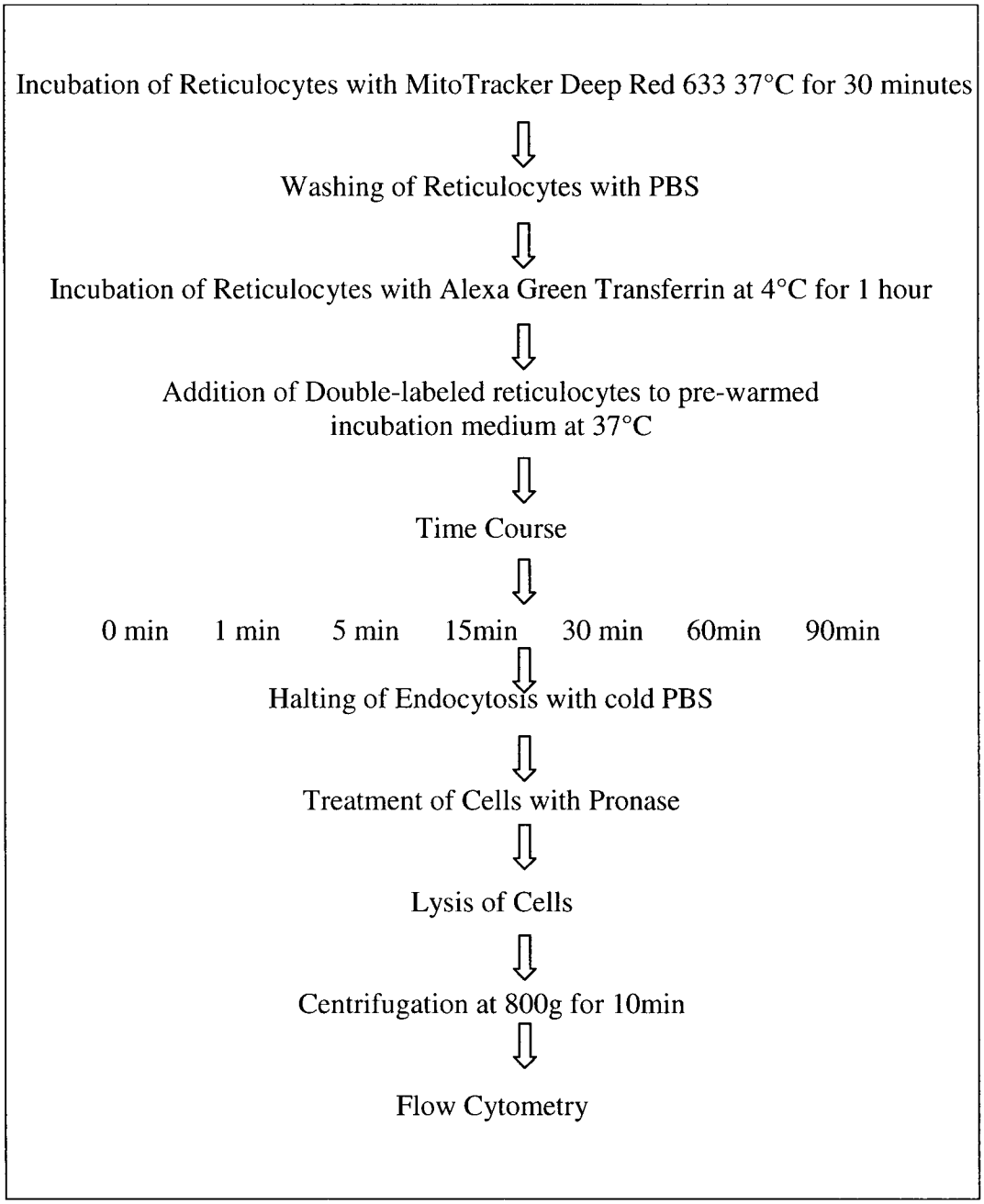

Figure 6- Time Course of Double-Labeled Reticulocytes
Protocol for preparing doubly stained reticulocytes and for double label time course

A

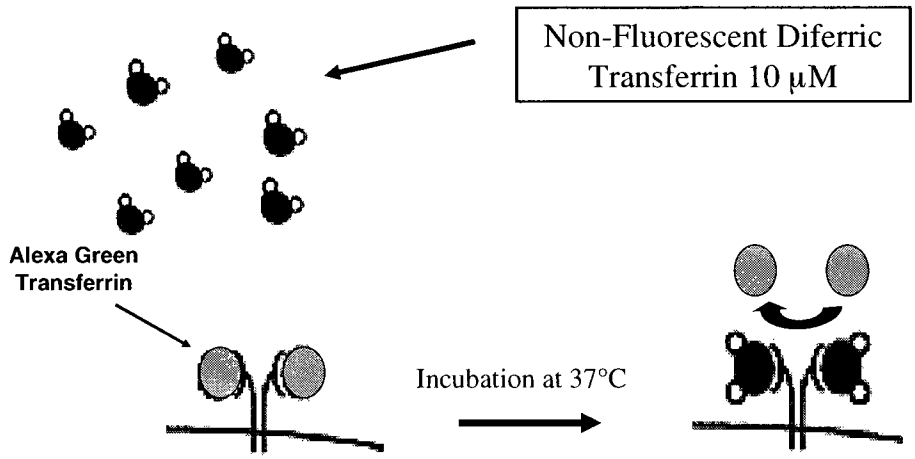

Transferrin Receptor

+

Alexa Green Transferrin

Transferrin Receptor

+

Non-Fluorescent Diferric Transferrin

B

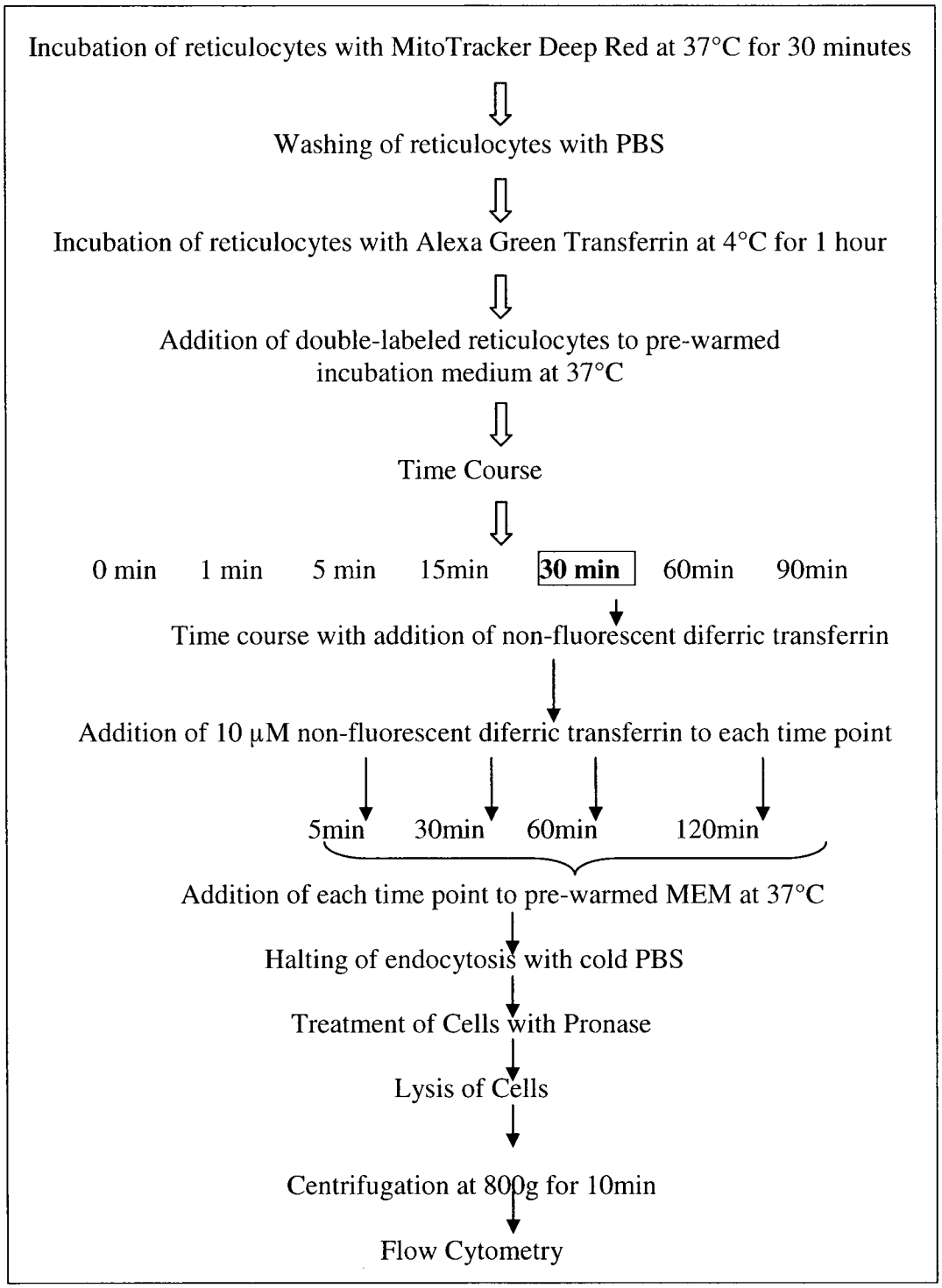

Figure 7–Treatment of Double-labeled Reticulocytes with Non-Fluorescent Diferric Transferrin

(A) Incubation of double-labeled reticulocytes at 37°C in the presence of 10 μM non-fluorescent diferric transferrin results in the exocytosis of Alexa Green Transferrin and the binding of non-fluorescent diferric transferrin to the

transferrin receptor. **(B)** Protocol for treatment of reticulocytes with non-fluorscent diferric transferrin

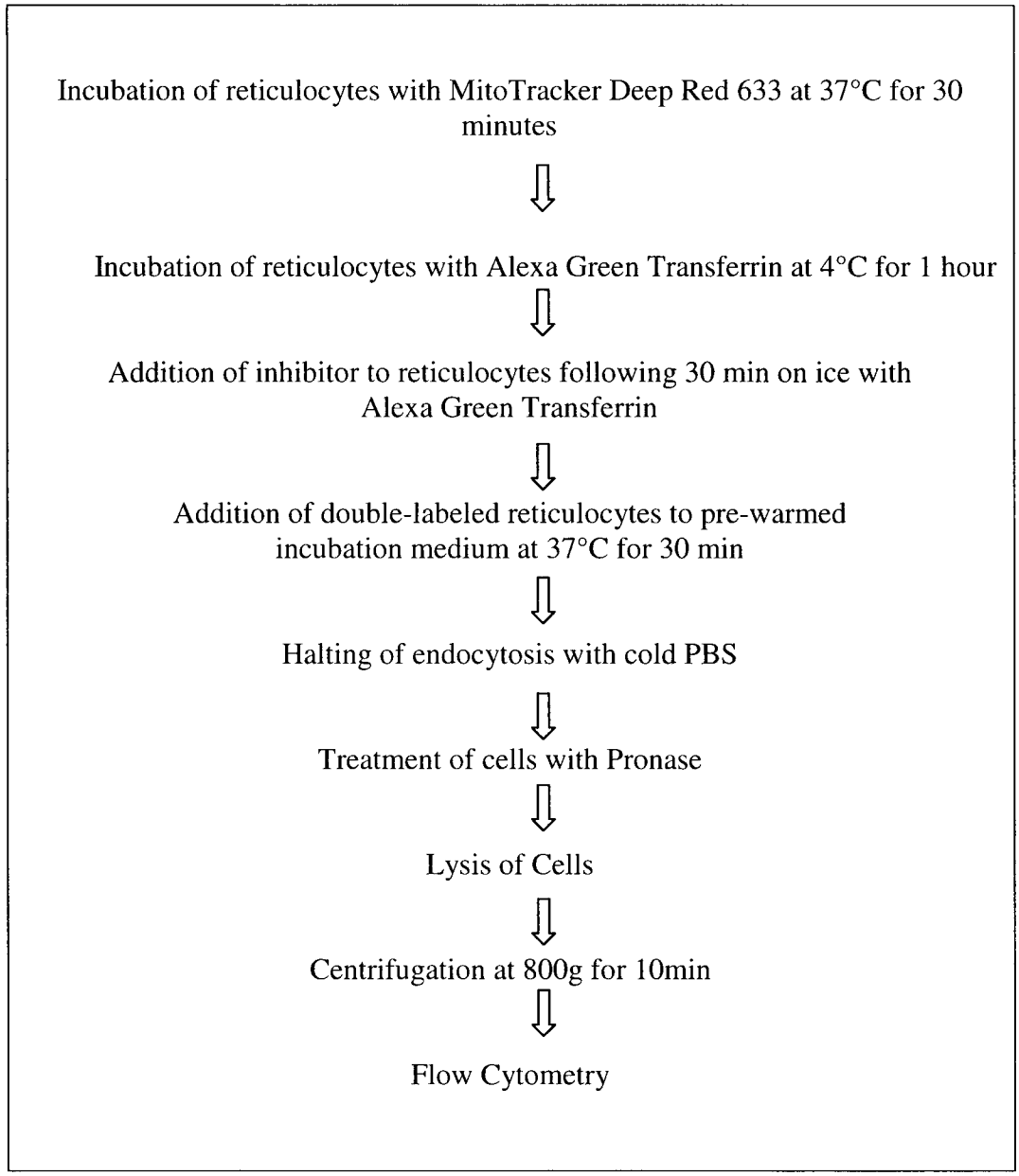

Figure 8 –Treatment of Reticulocytes with Inhibitors
Protocol for staining reticulocytes and treatment with inhibitors

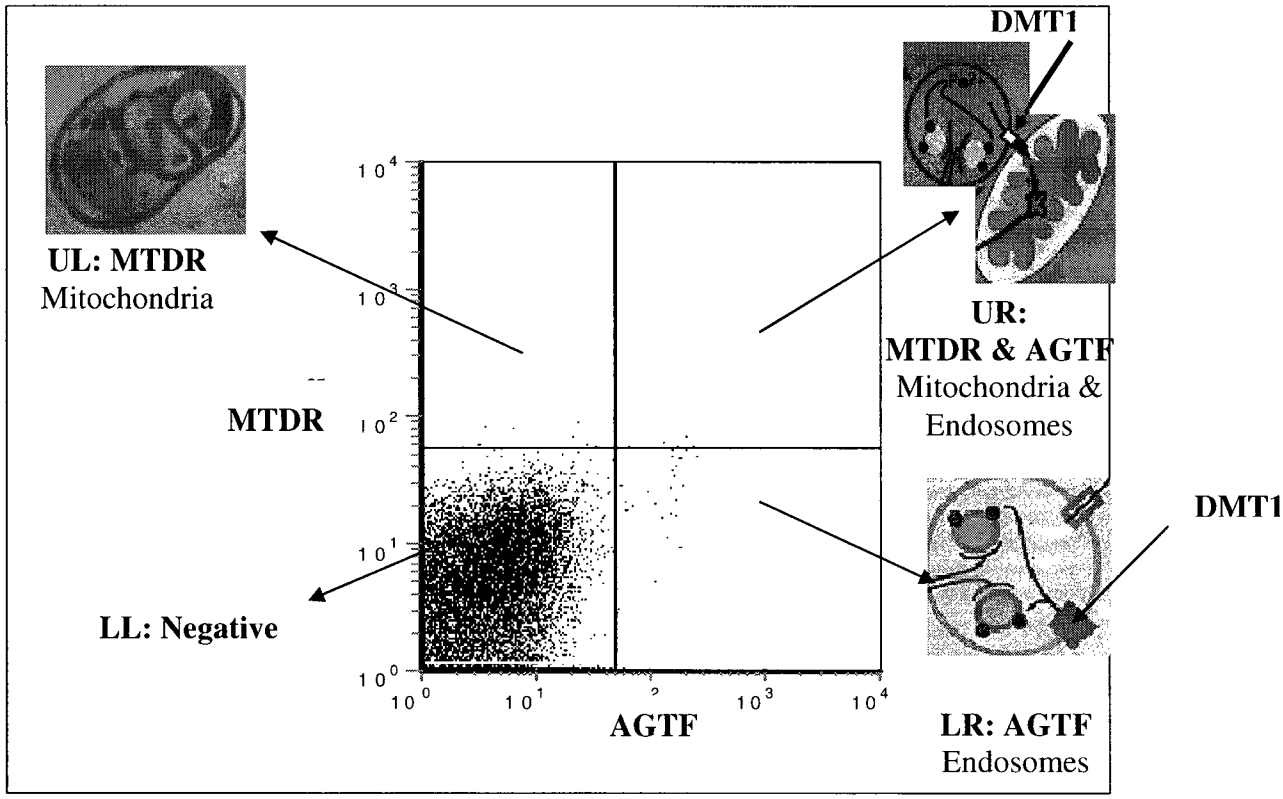

Figure 9. Endosomal & Mitochondrial Interaction Displayed by Flow Cytometry

The dot plot was subdivided into four quadrants: upper left (UL), upper right (UR), lower left (LL), and lower right (LR). Each quadrant represented specific populations. The UR quadrant represented events fluorescing both Alexa Green Transferrin (AGTF) and MitoTracker Deep Red (MTDR) and are referred to as the double labeled population. The UL quadrant displayed events labeled only with MTDR and therefore represented a mitochondrial population. The LR quadrant displayed events labeled only with AGTF and therefore represented an endosomal population. Lastly, the lower left (LL) quadrant displayed events devoid of all fluorescence. The double population of the UR quadrant suggests an association between endosomes and mitochondria. We postulate that iron transfer from the endosome to the mitochondria is facilitated via an interaction between divalent metal transporter 1 (DMT1) and an unknown mitochondrial protein.

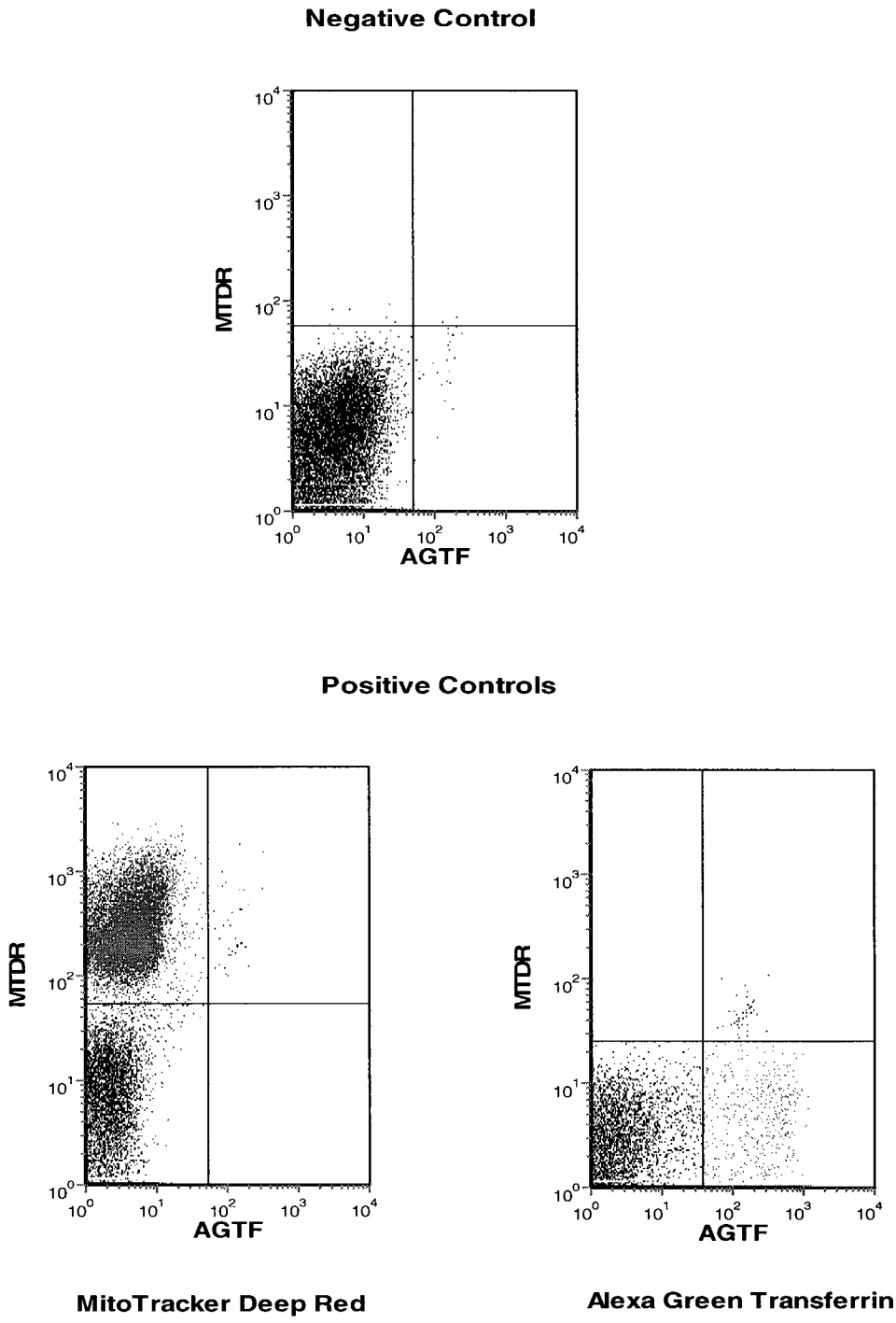

Figure 10. Flow Cytometry: Positive and Negative Controls

Reticulocytes were stained with either MitoTracker Deep Red (MTDR) or Alexa Green Transferrin (AGTF) for the positive control of each fluorophore. Reticulocytes used for the negative control were devoid of all fluorescence. Cells were lysed, centrifuged and the supernatant subjected to flow cytometry analysis.

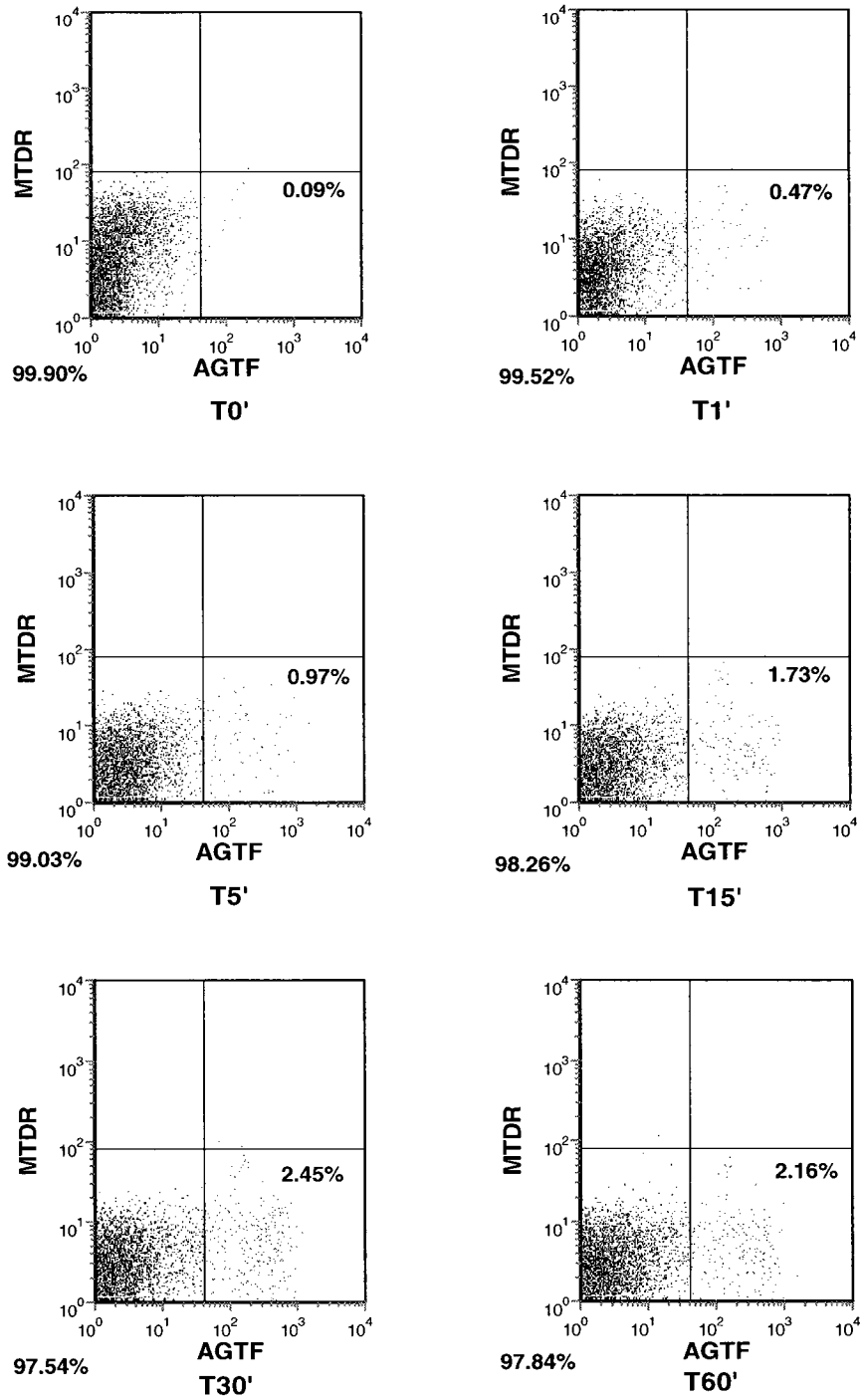

Figure 11. Percent of the Endosomal Population (LR quadrant) Increases with Time in Reticulocytes Labeled Solely with AGTF

Reticulocytes were labeled only with AGTF and incubated in pre-warmed incubation media for the indicated time. Cells were lysed and centrifuged; the supernatant was collected and analysed by flow cytometry. 50,000 events were analyzed via flow cytometry and are displayed in each dot plot. The number of events in each quadrant is represented as a percentage of the total number of events analyzed.

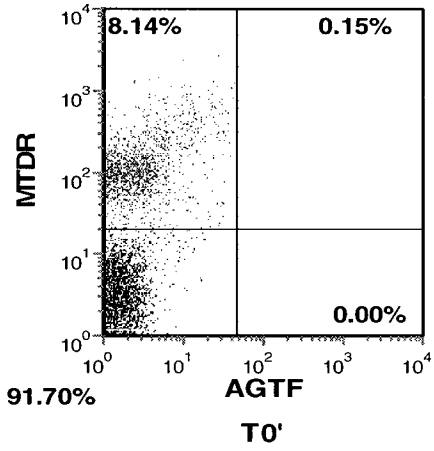
8.14%
0.15%
0.00%
91.70%
MTDR
AGTF
T0'

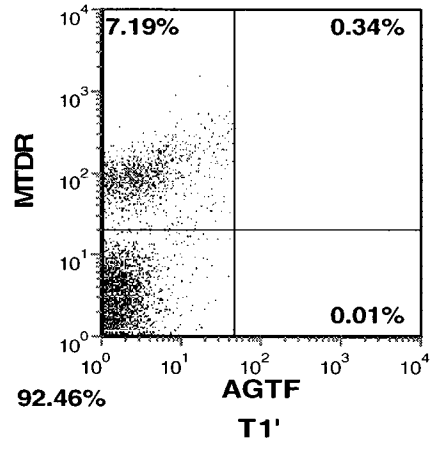
7.19%
0.34%
0.01%
92.46%
MTDR
AGTF
T1'

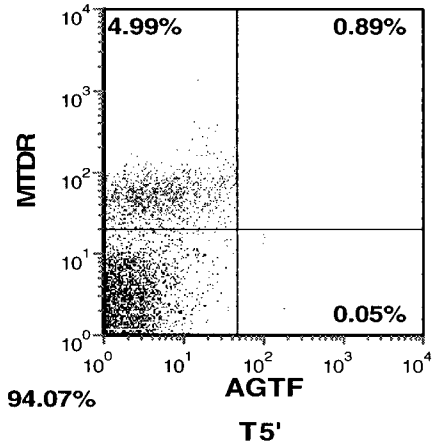
4.99%
0.89%
0.05%
94.07%
MTDR
AGTF
T5'

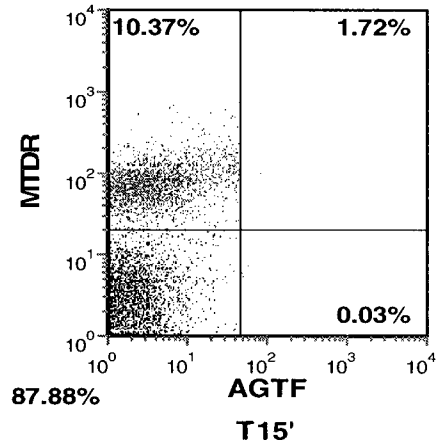
10.37%
1.72%
0.03%
87.88%
MTDR
AGTF
T15'

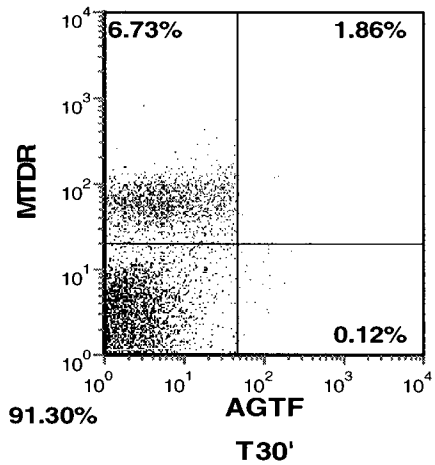
6.73%
1.86%
0.12%
91.30%
MTDR
AGTF
T30'

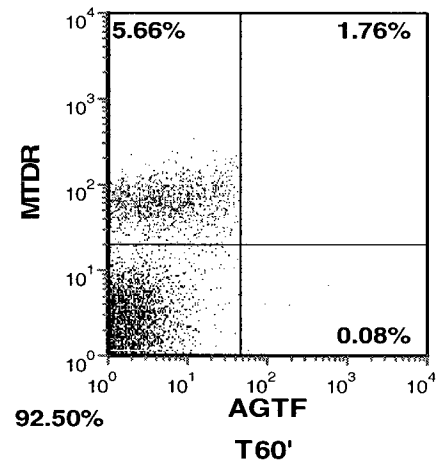
5.66%
1.76%
0.08%
92.50%
MTDR
AGTF
T60'

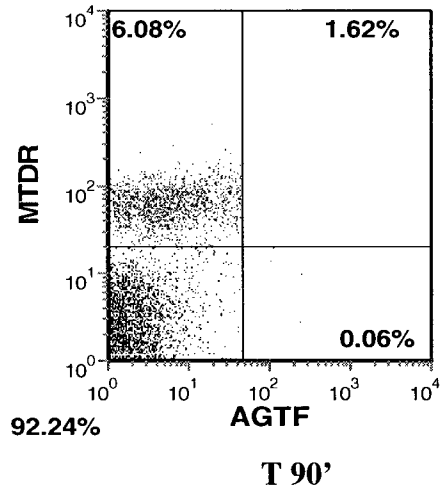

Figure 12. Percentage of Mitochondria Associated with Endosomes (UR quadrant) Increases with Time

Reticulocytes were labeled first with MitoTracker Deep Red (MTDR) and then Alexa Green Transferrin (AGTF). The doubly labeled reticulocytes were placed in pre-warmed incubation media for the indicated times. Following the incubation period, cells were lysed and were centrifuged. The supernatant of each time point was subjected to flow cytometry analysis. Once again, 50,000 events were processed. The number of events in each quadrant is represented as a percentage of the total number of events analyzed.

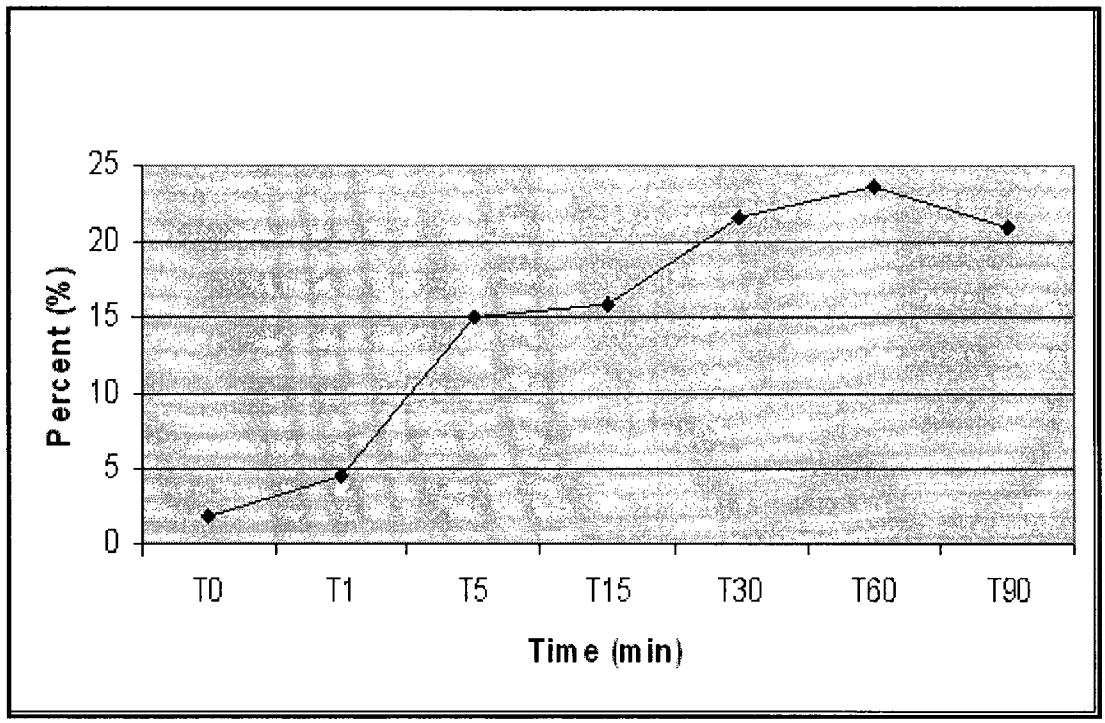

Figure 13. Percentage of Total Mitochondria Associated with Endosomes Increases with Time

Using data obtained from flow cytometry analysis, the percentage of total mitochondria associated with endosomes was calculated for each time point. The total number of mitochondria was represented as the sum of the events of the UL and UR quadrants which represented single mitochondria and mitochondria associated with endosomes respectively.

Percentage of total mitochondria associated with endosomes :

$$\% = \frac{UR}{(UL + UR)} \times 100$$

OR

$$\% = \frac{(\text{Mitochondria} + \text{Endosomes})}{\text{Mitochondria} + (\text{Mitochondria} + \text{Endosomes})} \times 100$$

A

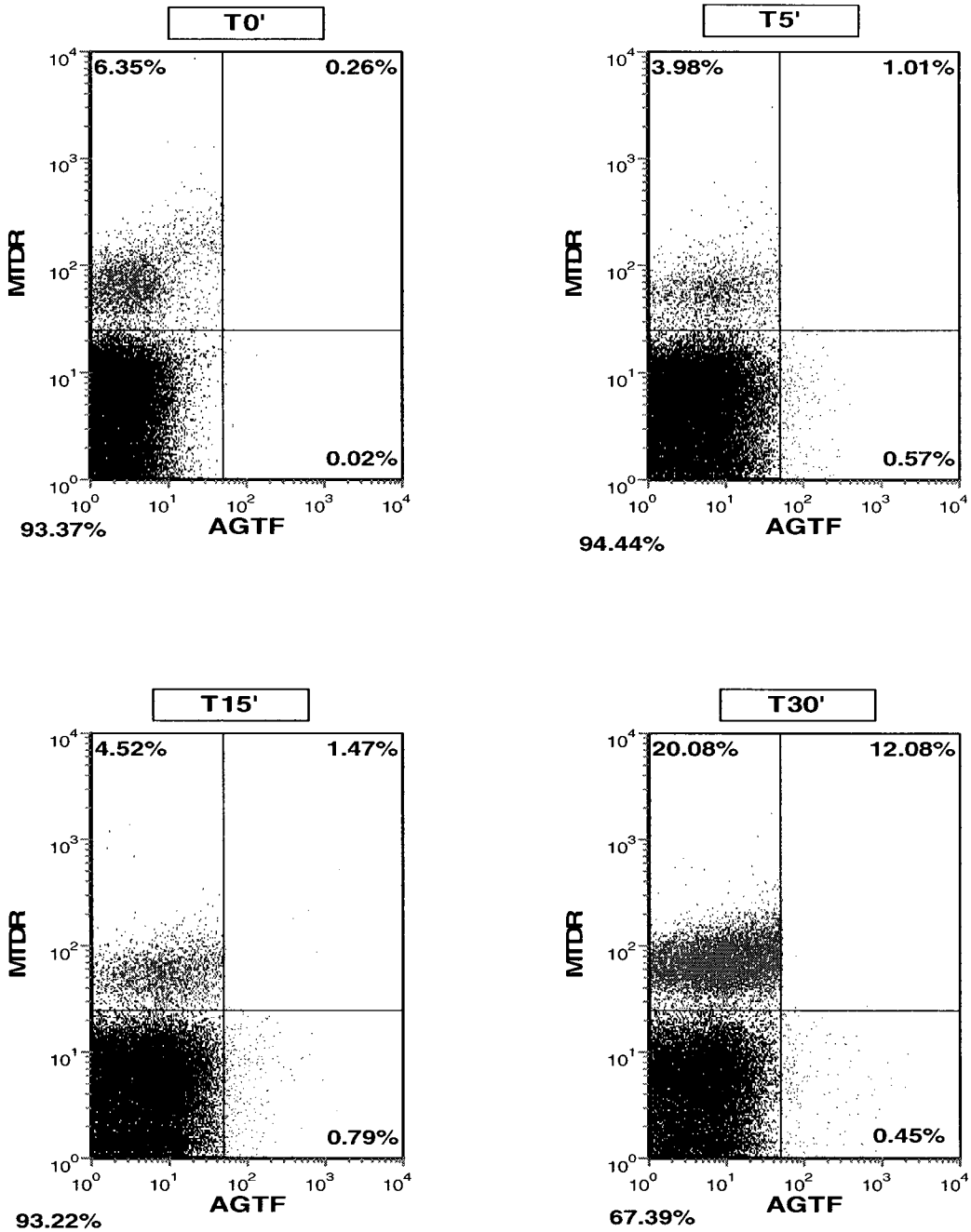
T0'
6.35%
0.26%
0.02%
93.37%
T5'
3.98%
1.01%
0.57%
94.44%
T15'
4.52%
1.47%
0.79%
93.22%
T30'
20.08%
12.08%
0.45%
67.39%
MTDR
AGTF

B

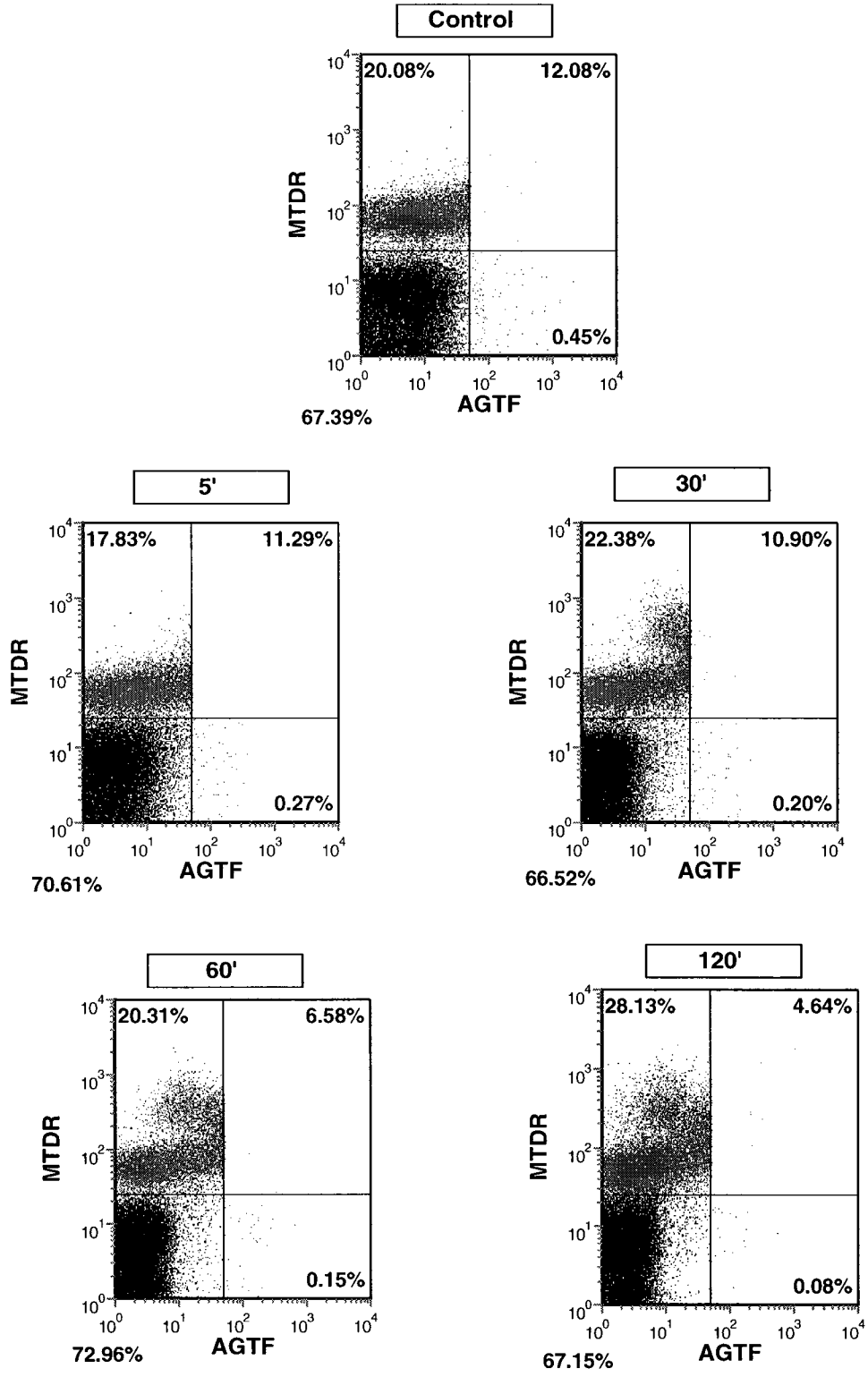
Control
20.08%
12.08%
0.45%
67.39%
MTDR
AGTF
5'
17.83%
11.29%
0.27%
70.61%
30'
22.38%
10.90%
0.20%
66.52%
60'
20.31%
6.58%
0.15%
72.96%
120'
28.13%
4.64%
0.08%
67.15%

Figure 14. Double-labeled Population (following procedure shown in figure 14) Can Be Dissociated by Treatment with Non-Fluorescent Diferric Transferrin

Reticulocytes were labeled first with MitoTracker Deep Red (MTDR) and then Alexa Green Transferrin (AGTF). **(A)** The doubly labeled reticulocytes were then placed in pre-warmed incubation media at 37°C for the indicated times. Following the incubation period of T30', the sample was resuspended and subdivided into the following time points: 5', 30', 60' and 120'. **(B)** Each time point was incubated in the presence of 10 uM non-fluorescent diferric transferrin at 37°C for the prescribed amount of time.

Cells were lysed and were centrifuged and the supernatant of each time point was analyzed via flow cytometry. Once again, 50,000 events were processed for each sample and are displayed in each dot plot. The number of events found in each quadrant is represented as a percentage of the total number of events analyzed.

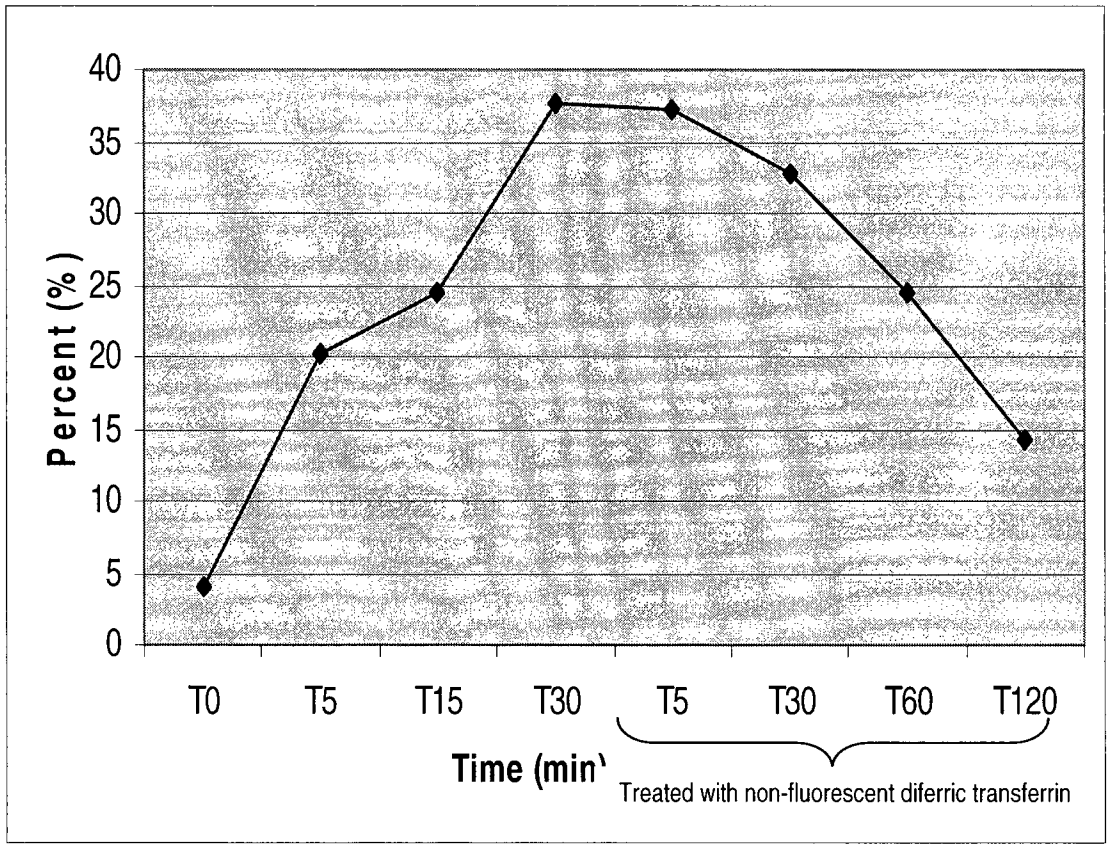

Figure 15. Treatment of Double-Labeled Reticulocytes with Non-Fluorescent Diferric Transferrin Results in a Decrease in the Percentage of Total Mitochondria Associated with Endosomes

Reticulocytes were labeled first with MitoTracker Deep Red (MTDR) and then Alexa Green Transferrin (AGTF). The doubly labeled reticulocytes were then placed in pre-warmed incubation media at 37°C for the indicated time. Following the incubation period of T30', the sample was resuspended and subdivided into the following time points: 5', 30', 60' and 120'. Each time point was incubated in the presence of 10 uM non-fluorescent diferric transferrin at 37°C for the indicated times. Cells were lysed and were centrifuged. The supernatant of each time point was analyzed via flow cytometry. The percentage of total mitochondria associated with endosomes at each time point was calculated as previously described in Figure 13.

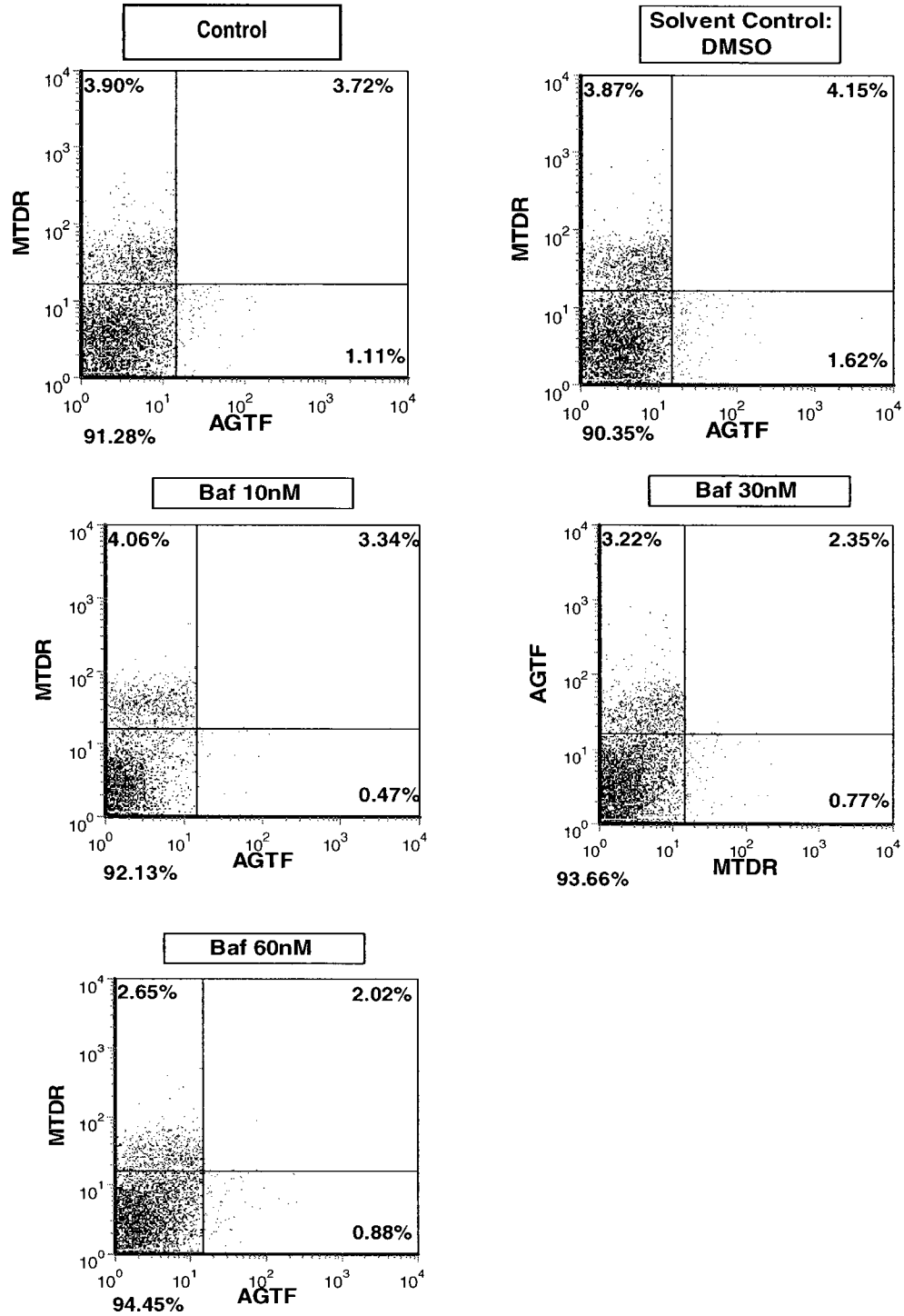

Figure 16. Treatment with Bafilomycin (Baf) Results in a Decrease in the Double-Labeled Population of the Upper Right (UR) Quadrant

Doubly labeled reticulocytes were incubated with Baf at the indicated concentrations for 30 minutes on ice followed by a 30 minute incubation at 37°C. Inhibitor was not added to the solvent control; instead the volume of DMSO added was equal to the maximum volume of inhibitor used. The inhibitor was not

added to the drug control; however the sample was subjected to both incubations at 4°C and 37°C. Cells were lysed and were centrifuged. The supernatant of each time point was analyzed via flow cytometry. Once again, 50,000 events were processed for each sample and are displayed in each dot plot. The number of events found in each quadrant is represented as a percentage of the total number of events analyzed.

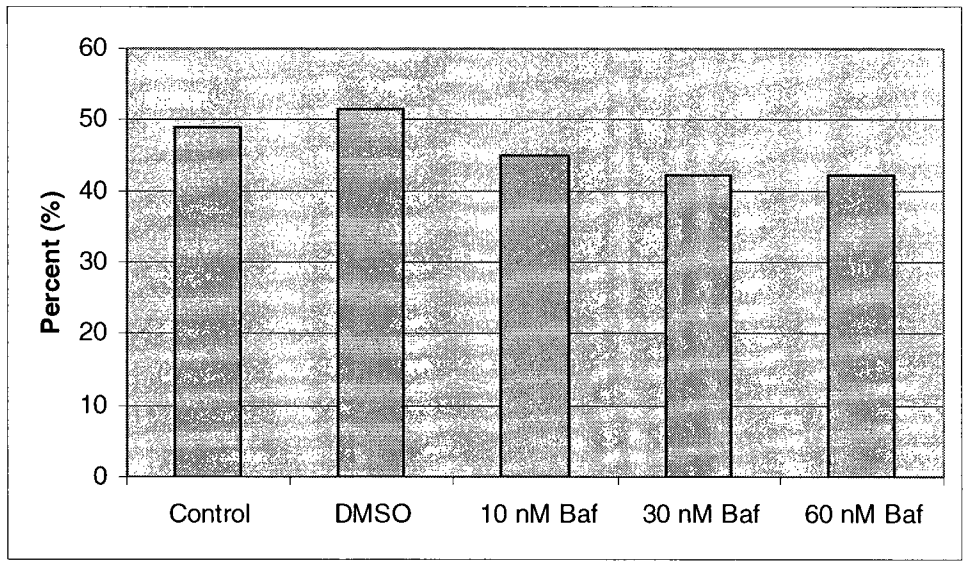

Figure 17. Treatment with Bafilomycin (Baf) Results in a Decrease in the Percentage of Total Mitochondria Associated with Endosomes

The percentage of total mitochondria associated with endosomes was calculated for each treatment. Percentages were calculated as previously described in Figure 13.

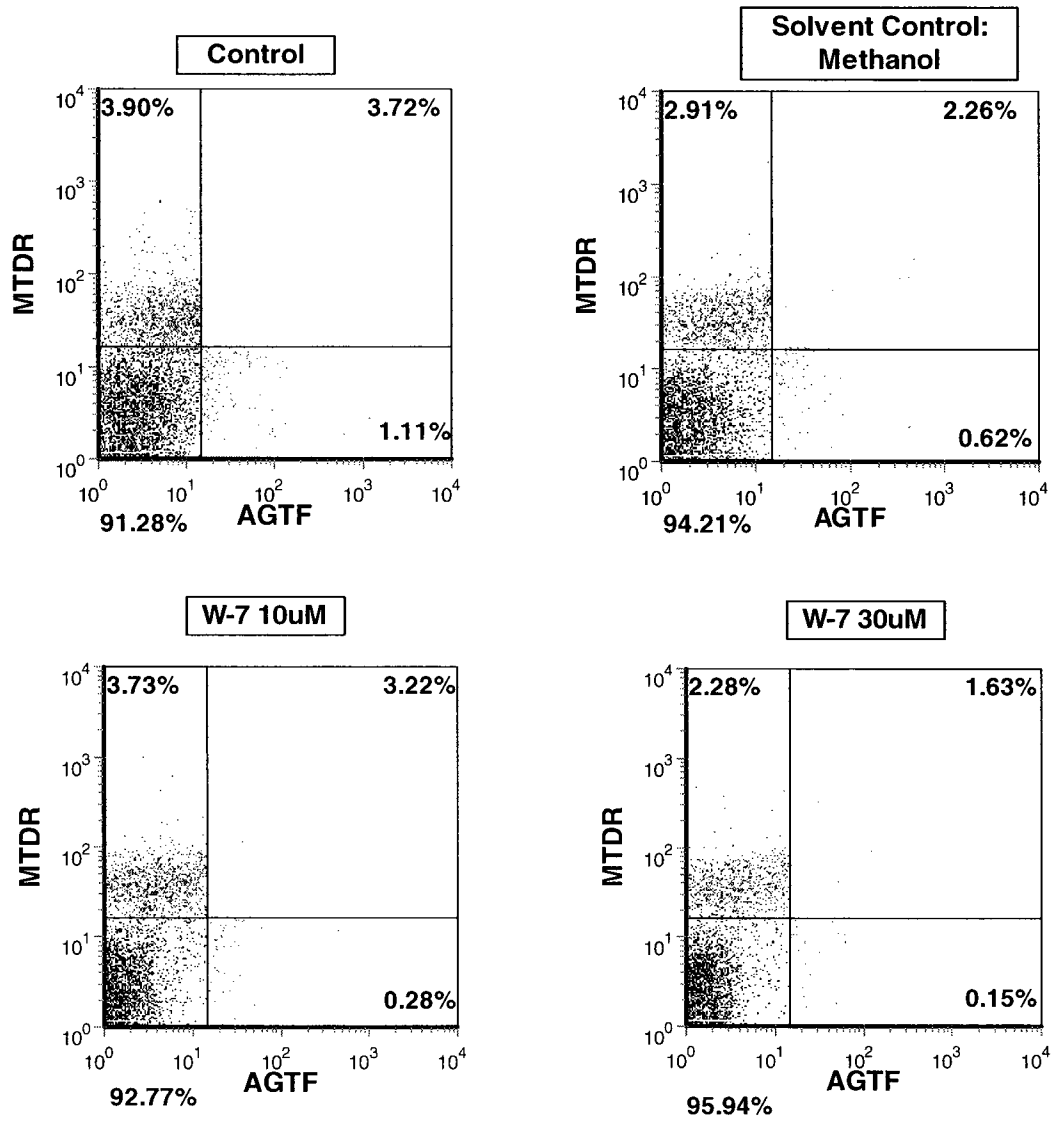

Figure 18. Treatment with W-7 results in a decrease in the double-labeled population of the upper right (UR) quadrant

Double labeled reticulocytes were incubated with W-7 at the indicated concentrations for 30 minutes on ice followed by a 30 minute incubation at 37°C. Inhibitor was not added to the solvent control; instead the volume of methanol added was equal to the maximum volume of inhibitor used. The inhibitor was not added to the drug control, however the sample was subjected to both incubations at 4°C and 37°C. Once again, 50,000 events were processed for each sample and are displayed in each dot plot. The number of events found in each quadrant is represented as a percentage of the total number of events analyzed.

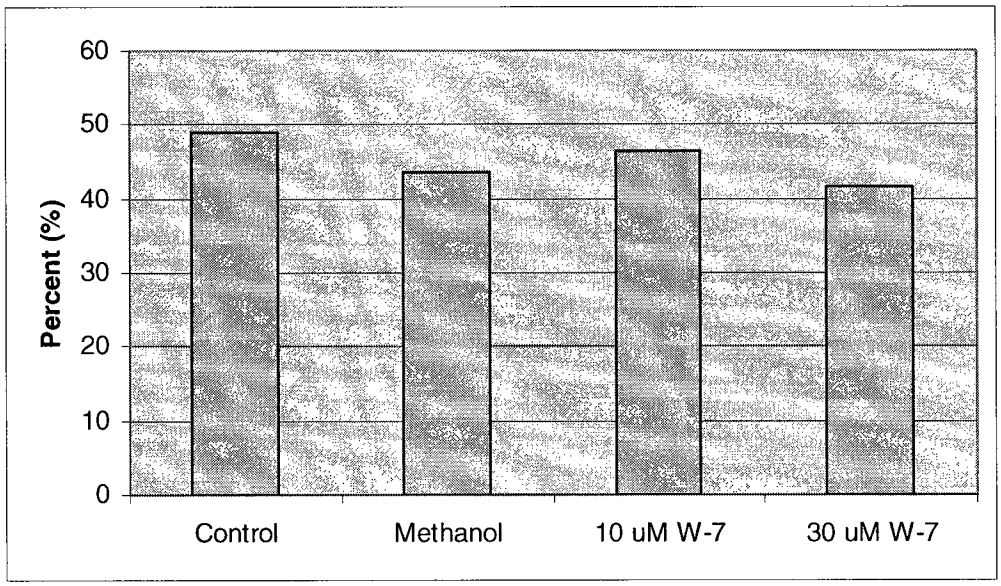

Figure 19. Treatment with W-7 Results in a Decrease in the Percentage of Total Mitochondria Associated with Endosomes

The percentage of total mitochondria associated with endosomes was calculated for each treatment. Percentages were calculated as previously described in Figure 13.

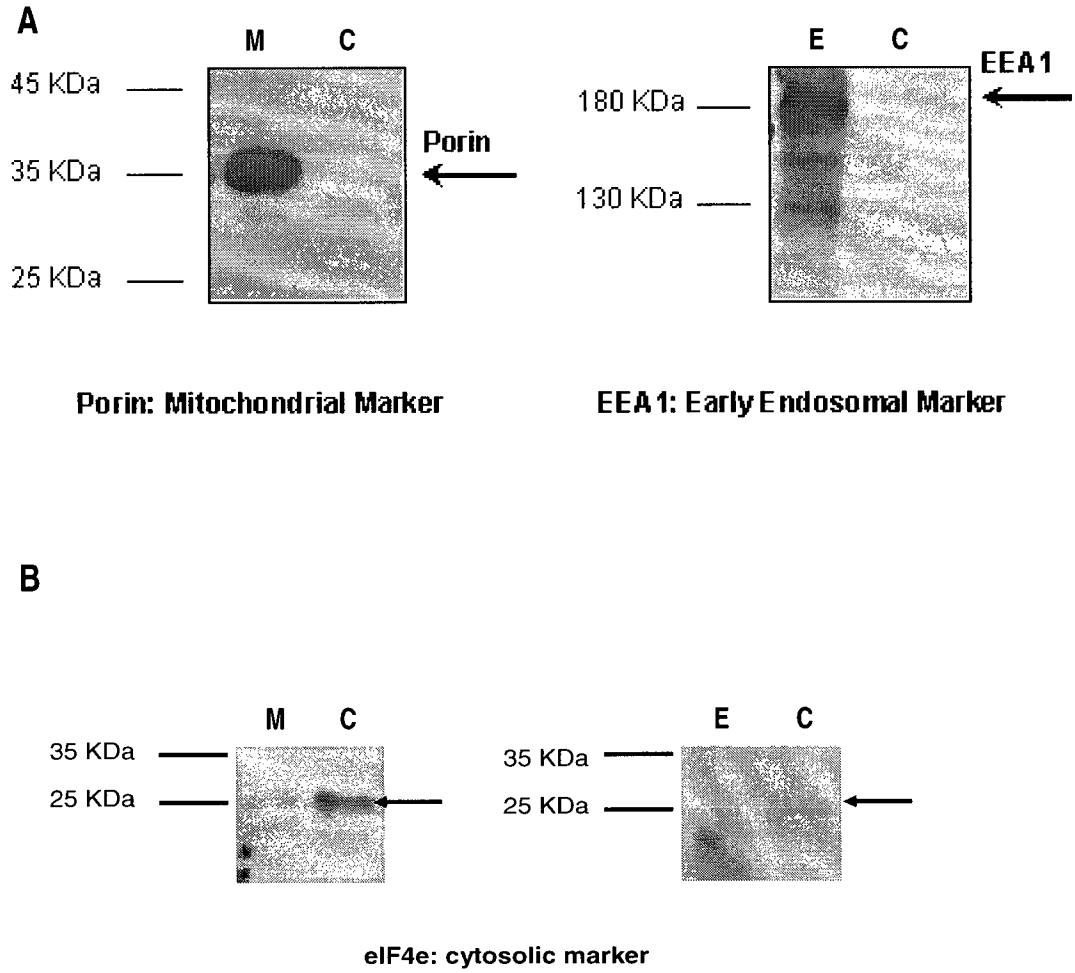

Figure 20. Isolation of Mitochondria and Endosomes from Erythroid Cells for Erythroid Cell-Free Assay

Mitochondria were isolated from splenic erythroblasts and endosomes from reticulocytes. 30 ug of isolated mitochondrial or endosomal protein and its cytosolic fraction were loaded per lane on a sodium dodecyl sulfate, 10% polyacrylamide gel and transferred to a nitrocellulose membrane. **(A)** Purity of the mitochondrial and endosomal fraction was verified with a polyclonal antibody specific to each organelle, Porin and EEA1 respectively. In order to determine cytosolic contamination in each organellar fraction, 30 ug of mitochondrial or endosomal protein was run on a 12% polyacrylamide gel and transferred to a nitrocellulose membrane. **(B)** Membranes were probed using eIF4e, a cytosolic marker. (M, mitochondria; E, endosome; C, cytosol)

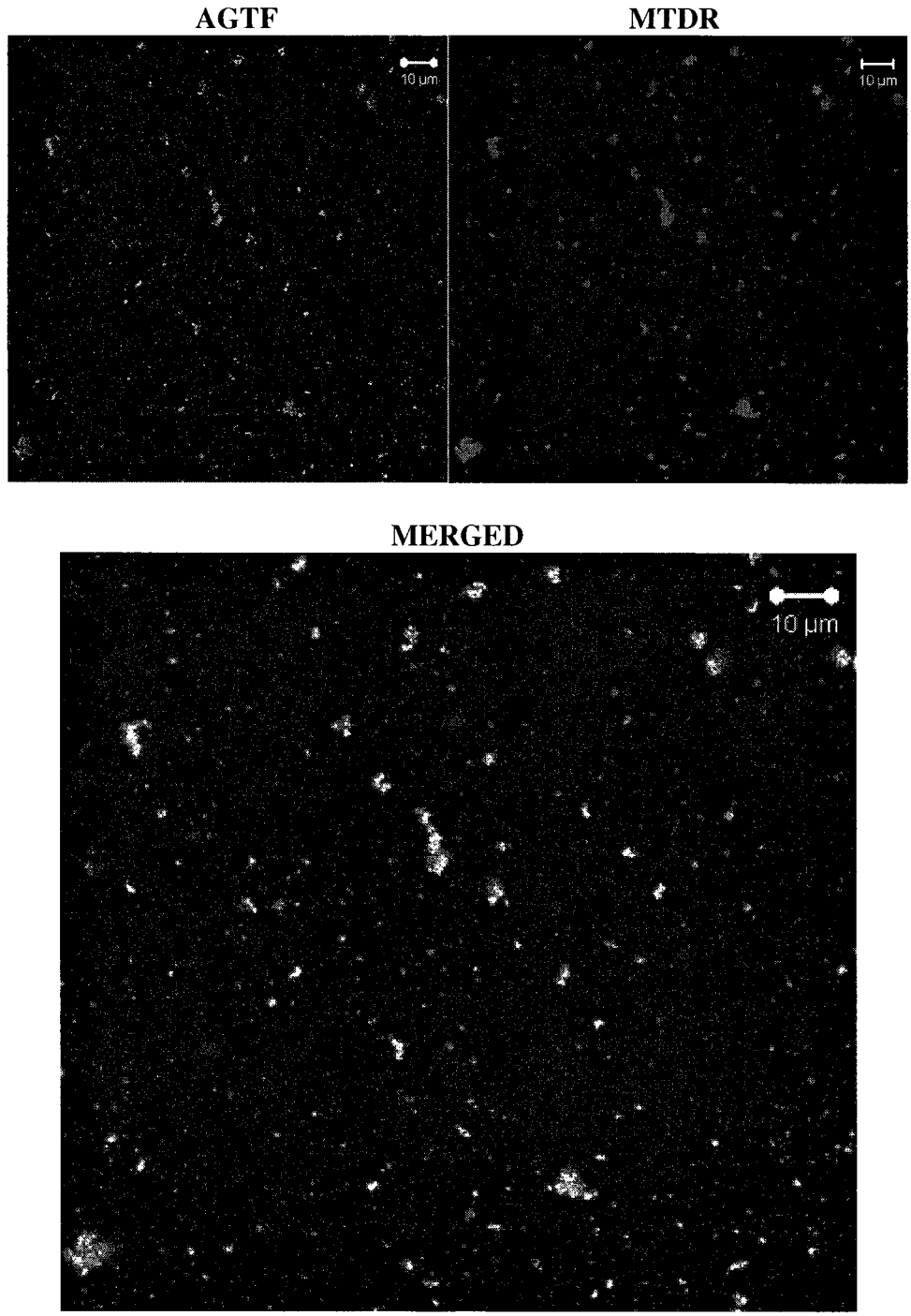

Figure 21. Mitochondria and Endosomes Colocalize in Erythroid Cell-Free Assay

Organelles were visualized by confocal microscopy. Mitochondria were isolated from spleenic erythroblasts and stained with MitoTracker Deep Red (MTDR). Endosomes were labeled with Alexa Green Transferrin (AGTF) and isolated from reticulocytes. Cell-free assay consisted of fluorescent mitochondria (red) and endosomes (green), ATP, GTP, and cytosol isolated from reticulocytes. The colocalization of the two fluorescent organelles is represented by the yellow signal.

A: Control

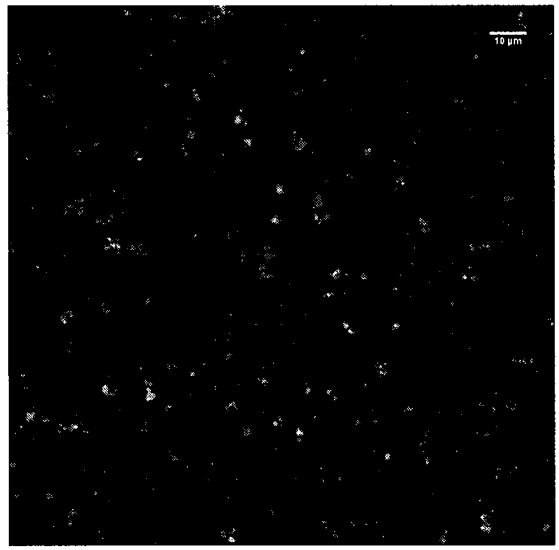

B: CCCP Treatment

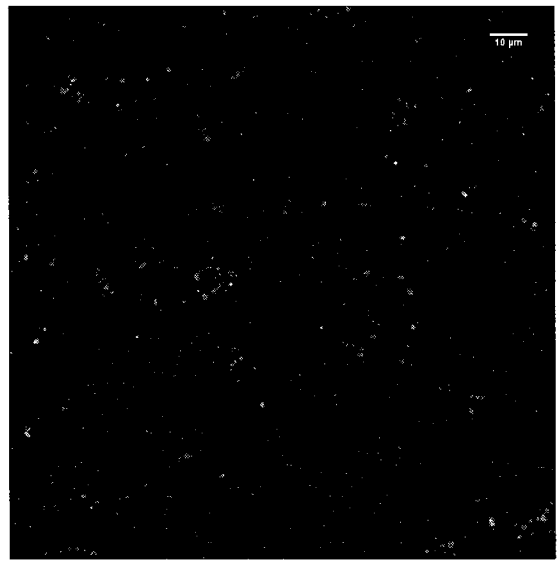

Figure 22. Treatment of HeLa Cell-Free Assay with Mitochondrial Uncoupler, CCCP, Results in a Decrease in Mitochondrial and Endosomal Association

Fluorescent mitochondria (red) and endosomes (green) were isolated from HeLa cells. Cell-free assay consisted of mitochondria, endosomes, ATP, GTP and cytosol isolated from HeLa cells. The assay was incubated for 15 minutes at 37°C. **(A)** The control sample was incubated in the absence of CCCP. **(B)** The uncoupler was added to the treated sample during the 15 minute incubation at a concentration of 4uM.

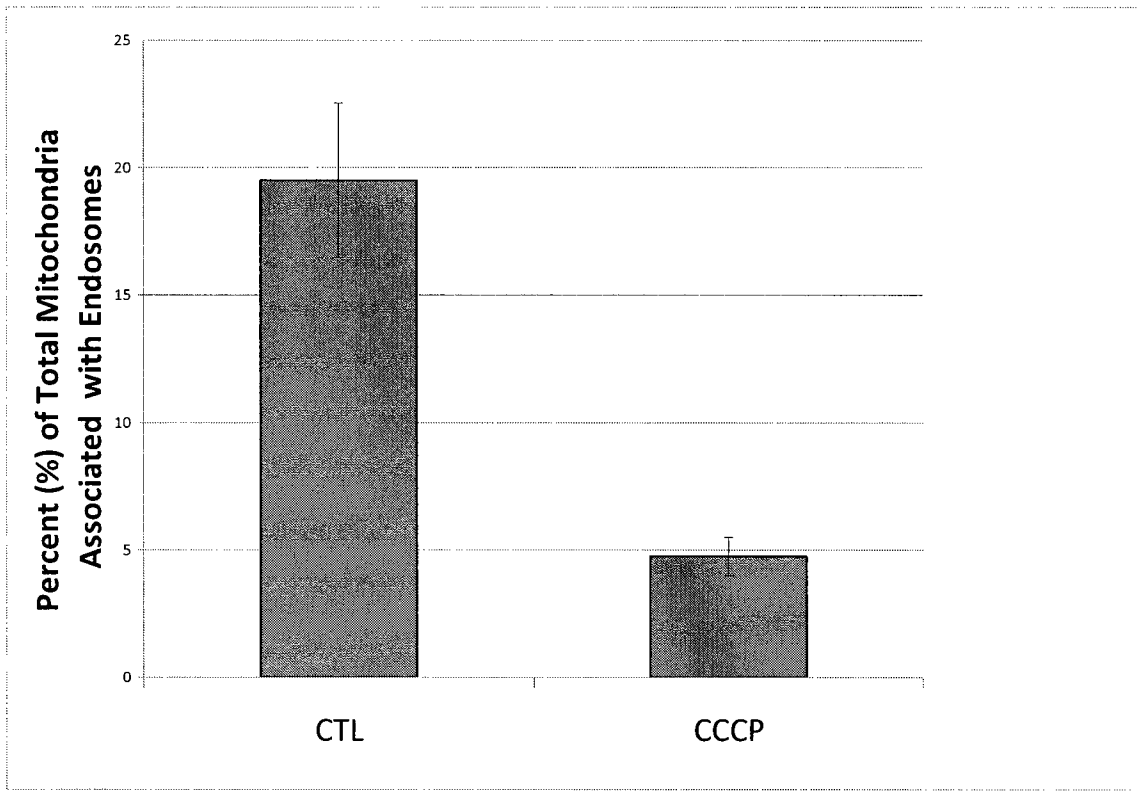

Figure 23. Treatment of HeLa Cell-Free Assay with CCCP Significantly Reduces Percent of Total Mitochondria Associated with Endosomes

In total 200 mitochondria were counted per sample and the number of mitochondria associated with endosomes was counted as well. The experiment was repeated three times and the difference noted between the control and CCCP-treated sample was deemed statistically significant ($p<0.0153$)

5 b) SPECIFIC OBJECTIVES OF THE STUDY: Summarize in point form the primary objectives of this study.

- To develop and test new iron chelating drugs
- To examine the efficacy of these chelators to prevent oxygen radical mediated cell damage
- To investigate the mechanisms by which nitric oxide, a newly discovered biological messenger, affects metabolism of iron in cells
- To study the mechanism and regulation of iron mobilization from tissue stores to plasma transferrin
- Elucidate the mechanism and regulation of iron mobilization from tissue stores (macrophages) to plasma transferrin

5 c) Indicate if and how the current goals differ from those in last year's application.

The goals do not differ from last year's application.

5 d) List the section / subsection numbers where significant changes have been made

No significant changes have been made.

5 e) KEYWORDS: Using keywords only, list the procedures used on animals (e.g. anaesthesia, breeding colony, injection IP, gavage, drug administration, major survival surgery, euthanasia by exsanguination, behavioural studies). For a more complete list of suggested keywords refer to Appendix 1 of the Guidelines (www.mcgill.ca/researchoffice/compliance/animal/forms).

IP injection of thioglycolate
Tissue harvested under general anesthesia
Euthanasia
Tail vein injection

6. Animals Use data for CCAC

6 a) Purpose of Animal Use (Check most appropriate one):

1. ☒ **Studies of a fundamental nature/basic research**
2. ☐ **Studies for medical purposes relating to human/animal diseases/disorders**
3. ☐ **Regulatory testing**
4. ☐ **Development of products/appliances for human/veterinary medicine**
5. **If for Teaching, use the Animal Use Protocol form for Teaching (www.mcgill.ca/researchoffice/compliance/animal/forms)**

6 b) Will field studies be conducted? NO ☒ YES ☐ If yes, complete "Field Study Form"
Will the project involve genetically altering animals? NO ☒ YES ☐ If yes, complete SOP #5 or #6
Will the project involve breeding animals? NO ☐ YES ☒ If breeding transgenics or knockouts, complete SOP#4

7. Animal Data

7 a) Please justify the need for live animals versus alternate methods (e.g. tissue culture, computer simulation)

Results from tissue culture do not match those from freshly isolated cells. Reasons for this are under active investigation.

7 b) Describe the characteristics of the animal species selected that justifies its use in the proposed study (consider characteristics such as body size, species, strain, data from previous studies or unique anatomic/physiological features)

Rats: consistency with previous experiments. Mice: Specifically lack heme oxygenase and Nramp1 which are thought to be important in the processes being studied.

7 c) Description of animals

Quality Control Assurance: To prevent introduction of infectious diseases into animal facilities, a health status report or veterinary inspection certificate may be required prior to receiving animals from all non-commercial sources or from commercial sources whose animal health status is unknown or questionable. Quarantine and further testing may be required for these animals.

If more than 6 columns are needed, please attach another page

	Sp/strain 1	Sp/strain 2	Sp/strain 3	Sp/strain 4	Sp/strain 5	Sp/strain 6

Species	Rat	Mouse (breeding)	Mouse	Mouse	Mouse	Mouse (breeding)
Supplier/Source	Charles River	LDI	LDI	Charles River	Charles River	McIntyre Medical Building
Strain	Sprague-Dawley	Hmox1-/-	C57BL/6J	C3H/H3J	129/Sv	129/Sv Nramp1-/-
Sex	both	both	both	F	F	both
Age/Wt	250g	all	6-12wks	8+ wks	8+ wks	all
# To be purchased	30	10	368	96	96	10
# Produced by in-house breeding	0	96	0	0	0	96
# Other (e.g.field studies)						
#needed at one time	5	4 (1+3)	10	10	10	4 (1+3)
# per cage	3	4	6	5	5	4
TOTAL# /YEAR	30	96 + 10 (for breeding)	368	96	96	96 + 10 (for breeding)

7 d) Explanation of Animal Usage: BASED ON THE EXPERIMENTAL OBJECTIVES OF THE PROJECT, describe the number of animals required for one year. Include information on experimental and control groups, # per group, and failure rates.

For breeding, specify how many adults are used, number of offspring produced, and how many offspring are used in experimental procedures.

The arithmetic explaining how the total of animals for each column in the table above is calculated should be made clear.
(Space will expand as needed)

Hmox1-/-, C57BL6 (natural Nramp1 mutant), C3H/H3J (Nramp1 wild type), and 129/Sv (wild type + Nramp1-/-) Mice:
Approximately 10-20 million macrophages are harvested from each mouse and 250 million macrophages are required / experiment (as with rats). This will require 24 mice / experiment (24 x 10-20 million = 240-480 million macrophages). We expect to perform 4 experiments per year to achieve statistical significance. Therefore, 24 mice / experiment x 4 experiments / year = 96 mice / year / strain. Mice that are not of desired genotype will be sacrificed following genotyping.

Chelator testing (C57BL/6J Mice):
Donor mice: 20 mice required to harvest sufficient RBCs for model thalassemic RBC preparation (1 ml blood / mouse x 20 mice = 20 ml blood = 10 ml packed cells = 3 ml packed cells after biotinylation and alpha-chain loading; 3 ml is sufficient for 48 recipient mice) x 4 experiments / year = 80 mice subtotal.
Recipient mice: n = 6 x (3 control groups + 5 experimental groups) x 4 experiments / year = 192 mice subtotal.
80 donor mice + 192 recipient mice = 272 mice total / year.

8. Animal Husbandry and Care

8 a) If projects involves non-standard cages, diet and/or handling, please specify

8 b) Is there any component to the proposed procedures which will result in immunosuppression or decreased immune function (e.g. stress, radiation, steroids, chemotherapeutics, genetic modification of the immune system)?

NO ☒ YES ☐ if yes, specify:

8 c) Indicate area(s) where animal use procedures will be conducted:

Building: Lady Davis Institue **Room:** Animal Quarters

Indicate area(s) all facilities where animals will be housed:

Building: Lady Davis Institute **Room:** Animal Quarters

If animal housing and animal use are in different locations, briefly describe procedures for transporting animals:

9. Standard Operating Procedures (SOPs)

Complete this section if you plan to use any of the UACC SOPs listed below. IT IS UACC POLICY THAT THESE SOPS BE USED WHEN APPLICABLE. Any proposed variation of the SOPs must be described and justified. The Standard Operating Procedures can be found at the UACC website at www.mcgill.ca/researchoffice/compliance/animal/procedures . The completed and signed SOP form must be attached to the protocol.

Check all SOPs that will be used:

Blood Collection UACC#1	☒	Collection of Amphibian Oocytes UACC#9	☐
Anaesthesia in rodents UACC#2	☒	Rodent Survival Surgery UACC#10	☒
Analgesia in rodents UACC#3	☐	Anaesthesia & Analgesia Neonatal Rodents UACC#11	☐
Breeding transgenics/knockouts UACC#4	☒	Stereotaxic Survival Surgery in Rodents UACC#12	☐
Transgenic Generation UACC#5	☐	Field Studies Form	☐
Knockout/in Generation UACC#6	☐	Phenotype Disclosure Form	☐
Production of Monoclonal Antibodies UACC#7	☐	Other, specify:	☐
Production of Polyclonal Antibodies UACC#8	☐		☐

10. Description of Procedures

10 a) . IF A PROCEDURE IS COVERED BY AN SOP, WRITE "AS PER SOP", NO FURTHER DETAIL IS REQUIRED.

FOR EACH EXPERIMENTAL GROUP, DESCRIBE ALL PROCEDURES AND TECHNIQUES, WHICH ARE NOT PART OF THE SOPs, IN THE ORDER IN WHICH THEY WILL BE PERFORMED – surgical procedures, immunizations, behavioural tests, immobilization and restraint, food/water deprivation, requirements for post-operative care, sample collection, substance administration, special monitoring, etc Appendix 2 of the Guidelines (www.mcgill.ca/researchoffice/compliance/animal/guidelines) provides a sample list of points that should be addressed in this section.

Rats: The animals are injected with thioglycollate once daily for 3 consecutive days (1 ml of 3% thioglycolate IP) to increase the level of macrophages in the peritoneal cavity. three days after the final injection the animals are anesthetized (halothane). peritoneal macrophages isolated and used for in vitro experiments. The animals are then killed by anesthetic overdose. The animals will be monitored for distress and dead animals will be examined for the presence of adhesions.

Mutant Mice: As described above (with dose adjusted on a per weight basis), peritoneal macrophages will be isolated from Hmox1-/- and Nramp1 -/- mice and used for in vitro experiments.

10 b) Experimental endpoint – for each experimental group indicate survival time

Rats and mice will be sacrificed 6 days following the first thioglycollate injection.

10 c) Clinical endpoint – describe the conditions, complications, and criteria (e.g. >20% weight loss, maximum tumour size, vocalizing, lack of grooming) that would lead to euthanasia of an animal before the expected completion of the experiment (specify per species and project if multiple projects involved)

Mice will be monitored daily for lack of grooming, inability to eat or drink, >20% weight loss, behavioural abnormalities and signs of toxicity. Animals in distress will be euthanized immediately by carbon dioxide inhalation as per SOP # UACC-13.

Frequency of monitoring: Daily

10 d) Specify person(s) who will be responsible for animal monitoring and post-procedural care ***(must also be listed in section 4)***

Name: Matthias Schranzhofer	Phone #: 514-340-8222 ext. 5289

10 e) Pre-Anesthetic/Anaesthetic/Analgesic Agents: List all drugs that will be used to minimize pain, distress or discomfort. *(Table will expand as needed)*

Indicate area(s) all facilities where animals will be housed:

Building: Lady Davis Institute Room: Animal Quarters

If animal housing and animal use are in different locations, briefly describe procedures for transporting animals:

9. Standard Operating Procedures (SOPs)

Complete this section if you plan to use any of the UACC SOPs listed below. IT IS UACC POLICY THAT THESE SOPS BE USED WHEN APPLICABLE. Any proposed variation of the SOPs must be described and justified. The Standard Operating Procedures can be found at the UACC website at www.mcgill.ca/researchoffice/compliance/animal/procedures . The completed and signed SOP form must be attached to the protocol.

Check all SOPs that will be used;

Blood Collection UACC#1	☒	Collection of Amphibian Oocytes UACC#9	☐
Anaesthesia in rodents UACC#2	☒	Rodent Survival Surgery UACC#10	☒
Analgesia in rodents UACC#3	☐	Anaesthesia & Analgesia Neonatal Rodents UACC#11	☐
Breeding transgenics/knockouts UACC#4	☒	Stereotaxic Survival Surgery in Rodents UACC#12	☐
Transgenic Generation UACC#5	☐	Field Studies Form	☐
Knockout/in Generation UACC#6	☐	Phenotype Disclosure Form	☐
Production of Monoclonal Antibodies UACC#7	☐	Other, specify: 13	☒
Production of Polyclonal Antibodies UACC#8	☐		☐

10. Description of Procedures

10 a). IF A PROCEDURE IS COVERED BY AN SOP, WRITE "AS PER SOP", NO FURTHER DETAIL IS REQUIRED.

FOR EACH EXPERIMENTAL GROUP, DESCRIBE ALL PROCEDURES AND TECHNIQUES, WHICH ARE NOT PART OF THE SOPs, IN THE ORDER IN WHICH THEY WILL BE PERFORMED – surgical procedures, immunizations, behavioural tests, immobilization and restraint, food/water deprivation, requirements for post-operative care, sample collection, substance administration, special monitoring, etc Appendix 2 of the Guidelines (www.mcgill.ca/researchoffice/compliance/animal/guidelines) provides a sample list of points that should be addressed in this section.

Rats: The animals are injected with thioglycolate once daily for 3 consecutive days (1 ml of 3% thioglycolate IP) to increase the level of macrophages in the peritoneal cavity. three days after the final injection the animals are anesthetized (halothane). peritoneal macrophages isolated and used for in vitro experiments. The animals are then killed by anesthetic overdose. The animals will be monitored for distress and dead animals will be examined for the presence of adhesions.

Mutant Mice: As described above (with dose adjusted on a per weight basis), peritoneal macrophages will be isolated from Hmox1-/- and Nramp1 -/- mice and used for in vitro experiments.

129Sv Mice (Nramp1 wild-type and mutant): Mice will be anesthetized with isofluorane, splenectomized. and allowed to recover fully for 14 days as per SOP. Wounds will be closed with wound clips. Animals will be monitored daily for distress.

10 b) Experimental endpoint – for each experimental group indicate survival time

Rats and mice will be sacrificed 6 days following the first thioglycollate injection.

10 c) Clinical endpoint – describe the conditions, complications, and criteria (e.g. >20% weight loss, maximum tumour size, vocalizing, lack of grooming) that would lead to euthanasia of an animal before the expected completion of the experiment (specify per species and project if multiple projects involved)

Mice will be monitored daily for lack of grooming, inability to eat or drink, >20% weight loss, behavioural abnormalities and signs of toxicity. Animals in distress will be euthanized immediately by carbon dioxide inhalation as per SOP # UACC-13.

Frequency of monitoring: Daily

10 d) Specify person(s) who will be responsible for animal monitoring and post-procedural care *(must also be listed in*

(New page 30 MAI 2008)

Species	Agent	Dosage (mg/kg)	Total volume(ml) per administration	Route	Frequency/Duration
rat	isofluorane	N/A	N/A	inhalation	N/A
mouse	avertin	0.5	0.2	IP	N/A

10 f) Administration of ALL other substances: List all non-anaesthetic agents under study in the experimental component of the protocol, including but not limited to drugs, infectious agents, viruses. *(Table will expand as needed)*

Species	Agent	Dosage (mg/kg)	Total volume(ml) per administration	Route	Frequency/Duration
rat	thioglycollate	0.12	1 mL	IP	1/day for 3 days
mouse	thioglycollate	0.12	0.5 mL	IP	1/day for 3 days

10 g) Method of Euthanasia

Specify Species

- ☐ Anaesthetic overdose, list agent/dose/route:
- ☐ Exsanguination with anaesthesia, list agent/dose/route:
- ☐ Decapitation without anaesthesia *
- ☐ Decapitation with anesthesia, list agent/dose/route (including CO_2):
- ☐ Cervical dislocation without anaesthesia *
- ☒ Cervical dislocation with anaesthesia, list agent/dose/route (including CO_2):
- ☑ CO_2 chamber only
- ☐ Other, specify:
- ☐ Not applicable, explain:

* For physical method of euthanasia without anaesthesia, please justify:

11. Category of Invasiveness: B ☐ C ☒ D ☐ E ☐

Categories of Invasiveness (from the CCAC *Categories of Invasiveness in Animal Experiments*). Please refer to this document for a more detailed description of categories.

Category A: Studies or experiments on most invertebrates or no entire living material.

Category B: Studies or experiments causing little or no discomfort or stress. *These might include holding animals captive, injection, percutaneous blood sampling, accepted euthanasia for tissue harvest, acute non-survival experiments in which the animals are completely anaesthetized.*

Category C: Studies or experiments involving minor stress or pain of short duration. *These might include cannulation or catheterizations of blood vessels or body cavities under anaesthesia, minor surgery under anaesthesia, such as biopsy; short periods of restraint, overnight food and/or water deprivation which exceed periods of abstinence in nature; behavioural experiments on conscious animals that involve short-term stressful restraint.*

Category D: Studies or experiments that involve moderate to severe distress or discomfort. *These might include major surgery under anaesthesia with subsequent recovery, prolonged (several hours or more) periods of physical restraint; induction of behavioural stresses, immunization with complete Freund's adjuvant, application of noxious stimuli, procedures that produce pain, production of transgenics (in accordance with University policy).*

Category E: Procedures that involve inflicting severe pain, near, at or above the pain threshold of unanaesthetized, conscious animals. *Not confined to but may include exposure to noxious stimuli or agents whose effects are unknown; exposure to drugs or chemicals at levels that (may) markedly impair physiological systems and which cause death, severe pain or extreme distress or physical trauma on unanaesthetized animals.* According to University policy, E level studies are not permitted.

12. Potential Hazards to Personnel and Animals It is the responsibility of the investigator to obtain the necessary Biohazard and/or Radiation Safety permits before this protocol is submitted for review.

A copy of these certificates must be attached, if applicable.

No hazardous materials will be used in this study ☐

12 a) Indicate which of the following will be used in animals:

☐ Toxic chemicals ☐ Radioisotopes ☐ Carcinogens
☐ Infectious agents (includes vectors) ☐ Transplantable tumours and/or tissues

12 b) Complete the following table for each agent to be used (use additional page as required):

Agent name			
Dosage			
Route of administration			
Frequency of administration			
Duration of administration			
Number of animals involved			
Survival time after administration			

12 c) After administration the animals will be housed in:

☐ the animal care facility ☐ laboratory under supervision of laboratory personnel

Please note that cages must be appropriately labeled at all times.

12 d) Describe potential health risk (s) to humans or animals:

12 e) Describe measures that will be used to reduce risk to the environment and all project and animal facility personnel:

12 f) If using cell lines, have they been tested?

☐ Yes If yes, What human and/or animal pathogens have been tested?

☐ No If no, justify:

13. Reviewer's Comments and Modifications (to be completed by ACC only): The Animal Care Committee has made the following modification(s) to this animal use procedure protocol during the review process. Please make these changes to your copy and comply with the recommended changes as a condition of approval.